UCSF
UC San Francisco Previously Published Works

Title
Covalent Attachment of Heme to the Protein Moiety in an Insect E75 Nitric Oxide Sensor

Permalink
https://escholarship.org/uc/item/3tq6b4w8

Journal
Biochemistry, 51(37)

ISSN
0006-2960

Authors
Aicart-Ramos, Clara
Falcón, Margarita Valhondo
de Montellano, Paul R Ortiz
et al.

Publication Date
2012-09-18

DOI
10.1021/bi300848x

Peer reviewed

eScholarship.org Powered by the California Digital Library
University of California

NIH Public Access
Author Manuscript
Biochemistry. Author manuscript; available in PMC 2013 September 18.

Published in final edited form as:
Biochemistry. 2012 September 18; 51(37): 7403–7416. doi:10.1021/bi300848x.

Covalent attachment of heme to the protein moiety in an insect E75 nitric oxide sensor

Clara Aicart-Ramos[£], **Margarita Valhondo-Falcón**[¶], **Paul R. Ortiz de Montellano**[§], and **Ignacio Rodriguez-Crespo**[£,*]

[£]Departamento de Bioquímica y Biología Molecular I, Universidad Complutense, 28040, Madrid, Spain

[¶]Departamento de Química Orgánica, Universidad Complutense, 28040, Madrid, Spain

[§]Department of Pharmaceutical Chemistry, University of California, San Francisco, California 94158-2517, United States

Abstract

We have recombinantly expressed and purified the ligand binding domains (LBDs) of four insect nuclear receptors of the E75 family. The *Drosophila melanogaster* and *Bombyx mori* nuclear receptors were purified as ferric hemoproteins with Soret maxima at 424 nm, whereas their ferrous form had a Soret maximum at 425 nm that responds to ·NO and CO binding. In contrast, the purified LBD of *Oncopeltus fasciatus* displayed a Soret maximum at 415 nm for the ferric protein that shifted to 425 nm in its ferrous state. Binding of ·NO to the heme moiety of *D. melanogaster* and *B. mori* E75 LBD resulted in the appearance of a peak at 385 nm, whereas this peak appeared at 416 nm in the case of the *O. fasciatus* hemoprotein, resembling the behaviour displayed by its human homolog Rev-erbβ. HPLC analysis revealed that, unlike the *D. melanogaster* and *B. mori* counterparts, the heme group of *O. fasciatus* is covalently attached to the protein through the side-chains of two amino acids. The large sequence homology with *O. fasciatus* E75 led us to clone and express the LBD of *Blattella germanica*, which established that its spectral properties closely resemble those of *O. fasciatus* and that it also has the heme group covalently bound to the protein. Hence, ·NO/CO regulation of the transcriptional activity of these nuclear receptors might be differently controlled among various insect species. In addition, covalent heme binding provides strong evidence that at least some of these nuclear receptors function as diatomic gas sensors rather than heme sensors. Finally, our findings expand the classes of hemoproteins in which the heme group is normally covalently attached to the polypeptide chain.

Nuclear receptors, the largest superfamily of transcription factors, are ligand-regulated polypeptides that share common domain architecture. Binding of small molecules to the ligand binding domain (LBD) of nuclear receptors modulates their association to specific DNA motifs. In insects, the early-induced gene E75 has been implicated genetically in repression of several genes in the ecdysone-triggered cascade (1) and it is well-established that E75 also acts as a repressor in transient transfection assays (2–4). Heterodimerization of E75 with HR3 or SMRTER is known to block their ability to activate transcription (3, 5, 6). Interestingly, the *Drosophila melanogaster* E75 nuclear receptor, and more specifically its LBD, is a protein module that binds heme and diatomic gases such as ·NO and CO (3). Full-length *D. melanogaster* E75 is isolated as a heme-bound ferric hemoprotein when obtained from the insect pupae and its isolated LBD is also a hemoprotein when recombinantly expressed and purified from both bacteria and baculovirus-infected cells (3, 7, 8).

*Corresponding author: nacho@bbm1.ucm.es.

NIH-PA Author Manuscript
NIH-PA Author Manuscript
NIH-PA Author Manuscript

NIH-PA Author Manuscript

NIH-PA Author Manuscript

NIH-PA Author Manuscript

From a functional point of view, coordination of diatomic gases to the heme moiety of *D. melanogaster* E75 induces a conformational change that interferes with its interaction with HR3 and SMRTER nuclear receptors, discontinuing repression of their transcriptional activity (3, 6). Binding of ·NO to *D. melanogaster* E75 displaces the Cys and His axial ligands rendering a pentacoordinate Fe(II)NO hemoprotein and justifying the observation that ·NO functions as an antagonist of E75 repressor activity (3, 5, 6, 8). In flies, nitric oxide synthase-derived ·NO cancels the repression exerted by E75 on HR3 in the prothoracic gland (5). Furthermore, during the transition of larvae to prepupae, ·NO can almost completely inhibit the repressor activity of E75 by preventing its recruitment by SMRTER (6). Finally, CO binding to purified *D. melanogaster* E75 LBD produces a hexacoordinate Fe(II)CO complex with a sixth neutral ligand (7, 8), stabilizes the protein, and abrogates its interaction with an HR3 peptide (3) although it is not known if, in vivo, ferrous CO-bound *D. melanogaster* E75 LBD fails to bind to other nuclear receptors such as HR3 or SMRTER.

Within mammalian LBDs, the closest homologs of insect E75 are nuclear receptors Rev-erbα (NR1D1) and Rev-erbβ (NR1D2), two related proteins that generally act as transcriptional repressors, either on their own or recruiting co-repressor proteins (9). In most cases, Rev-erbs are present in the nucleus and bind as monomers to the Rev responsive element or as dimers to a Rev-RE direct repeat, RevDR-2 (10). As in the case of insect E75 LBDs, both Rev-erbα and Rev-erbβ bind heme and the reversible binding of heme seems to regulate Rev-erbβ transcription activity (11–13). Whereas wild-type Rev-erbβ can repress transcription of target genes, its His602Phe mutant, which is unable to bind heme, does not display this transcriptional repressor activity (12). Since heme cellular levels vary during the circadian cycle, Rev-erbα and Rev-erbβ are considered to link the circadian cycle and metabolism (14). Initially, it was proposed that the transcriptional activity of Rev-erbα or Rev-erbβ was not affected by reduction of the heme iron with sodium dithionite or by the addition of ·NO donors (12), although recent data suggest that both recombinant Rev-erbα and Rev-erbβ can indeed bind ·NO and CO (8, 13, 15). Moreover, heme-saturated Rev-erbβ can also bind ·NO, hence regulating the binding to co-repressors (13).

In this manuscript we have characterized the properties of four insect E75 LBDs. Purified recombinant E75 LBD from the silkworm *Bombyx mori* significantly resembles that of *Drosophila melanogaster*. Unexpectedly, we have observed that the heme moiety becomes covalently attached to large milkweed bug (*Oncopeltus fasciatus*) and German cockroach (*Blattella germanica*) E75 LBDs yielding proteins with spectral and functional properties that resemble those of Rev-erbα and Rev-erbβ rather than those of their *D. melanogaster* and *B. mori* counterparts. In hemoproteins, covalent attachment of the heme moiety to the protein is not without precedent. In cytochrome *c*, the heme moiety is covalently attached to the protein through thioether bonds between its two vinyl groups and the side-chains of two Cys residues (16). In the CYP4 family of cytochrome P450 enzymes, covalent attachment of the heme 5-methyl group to the side-chain of a Glu residue in helix I via an ester link has been observed in CYP4A, CYP4B and CYP4F proteins (17–21). In the case of lactoperoxidase and eosinophil peroxidase, the side-chains of a Glu and an Asp form ester links with the heme 1- and 5- methyl groups (22), respectively, whereas in myeloperoxidase, two types of linkages are found, one involving an ester link between the side-chains of Glu and Asp residues and the 1- and 5-methyl groups of heme, respectively, and the other a sulfonium link between the sulphur of a Met residue and the β-carbon of the heme 2-vinyl group (23). In cytochrome *c* peroxidase and ascorbate peroxidase, covalent linkages between the side-chain of a Trp residue and one of the vinyl groups of the heme moiety have been observed (24, 25).

NIH-PA Author Manuscript

NIH-PA Author Manuscript

NIH-PA Author Manuscript

Both the covalent attachment of heme and the various results reported herein have been interpreted in the light of the heme, CO, ·NO and redox sensing properties of this family of nuclear receptors.

Materials and methods

Materials

Buffers, chemicals, oligonucleotides, hemin and common laboratory reagents were obtained from Sigma-Aldrich if not otherwise indicated. *Pfu* polymerase, T4 DNA ligase, restriction endonucleases and Molecular Mass markers were obtained from Fermentas. Ni-NTA resin was from Qiagen. CO and ·NO gases were from Airgas. The RP523 *E. coli* strain deficient in heme biosynthesis was obtained from the Yale University genetic stock center. Fe(III) mesoporphyrin IX was purchased from Livchem (Mannheim, Germany).

cDNA of insect E75 LBDs

Drosophila melanogaster E75 LBD was retrieved by PCR from a cDNA preparation of fly embryos using oligonucleotides that matched the published sequence. The E75B LBD from *Oncopeltus fasciatus* was amplified by PCR using the complete cDNA extracted from embryos (18, 22, 26, 30 and 34 h) and was a gift from Dr. Deniz F. Erezyilmaz (Princeton University, USA) (26). The *Bombyx mori* E75A cDNA was a generous gift from Dr. Kostas Iatrou (Athens, Greece) (4). The cDNA of *Blattella germanica* E75A was provided by Dr. David Martin Casacuberta (Barcelona, Spain) (27).

Cloning of the insect E75 LBDs in the pCWori vector and site-directed mutagenesis

In all cases we used the NdeI (5′ end) and XbaI (3′ end) of the bacterial expression vector pCWori in which a hexa-His tag has been previously introduced in frame at the N-terminus end of the recombinant protein as previously described (28, 29). The DNA encoding *D. melanogaster* E75 LBD was amplified by PCR. A forward oligonucleotide (5′-ACCCAGAATCGCGGCCAGCAGCGAGCC-3′) and a reverse oligonucleotide (5′-GGGCGACTTGTTCTGCTGGCCATCGCTGTTG-3′) were first used to amplify the LBD (residues 341–604). A second PCR with *Pfu* polymerase using this template was performed using the oligonucleotides (5′-ACCCAGCATATGGGCCAGCAGCGAGCC-3′, NdeI site underlined) and (5′-, GGGCGACTTTCTAGACTAGCCATCGCTGTTG-3′, XbaI site underlined). Likewise, the DNA encoding the E75B LBD from *O. fasciatus* was amplified by PCR using the complete cDNA extracted from *O. fasciatus* embryos. A forward oligonucleotide (5′-GCAGAGCACCAACTCCAAGTGCCAGGAG-3′) and a reverse oligonucleotide (5′-CATTGAACCCCACATTTCGTGTTGCTG-3′) were first used to amplify the LBD (residues 88–348). A second PCR with *Pfu* polymerase was performed using the oligonucleotides (5′-GCAGAGCACCAACCATATGTGCCAGGAG-3′, NdeI site underlined) and (5′-CATTGAACTCTAGATTTCGTGTTGCTG-3′, XbaI site underlined). Site-directed mutagenesis was performed following the QuikChange mutagenesis protocol. The *O. fasciatus* Glu158 codon was changed for Lys and the Met245 codon for Thr.

Construction of the *D. melanogaster-O. fasciatus* chimeric proteins

After a Clustal comparison between *D. melanogaster* and *O. fasciatus* amino acid sequences (Fig. S2) we selected a stretch -TLLKAG- approximately in the middle of helix 5 in the LBD that was identical in both proteins. A silent AflII was introduced at this position by site-directed mutagenesis in both the *D. melanogaster* and *O. fasciatus* cDNA. Chimera *Dros/Onc* consisted in the combined N-terminus of *D. melanogaster* E75 LBD and the C-terminus of *O. fasciatus* E75. Chimera *Onc/Dros* consisted in the N-terminus of *O. fasciatus* E75 LBD and the C-terminus of *D. melanogaster* E75. The two chimeras were referred to as

NIH-PA Author Manuscript

NIH-PA Author Manuscript

NIH-PA Author Manuscript

chimera *Dros/Onc* (residues 341–446 of the *D. melanogaster* LBD followed by residues 194–348 of its *O. fasciatus* counterpart) and chimera *Onc/Dros* (residues 88–199 of the *O. fasciatus* LBD followed by residues 440–604 *D. melanogaster* counterpart). Both chimeric proteins were cloned and expressed in the pCWori vector.

Protein expression and purification

Recombinant protein expression was performed in the *E. coli* protease-deficient strain BL21(DE3). Cells were grown in 2XYT medium in the absence of hemin, to an OD600 of ~1 prior to induction for 18 h at 25°C by the addition of 1 mM IPTG. After centrifugation, the cell pellet was resuspended in 100 mM Tris-HCl (pH 7.0) plus lysozyme and protease inhibitors and lysed by sonication. All the E75 proteins expressed in *E. coli* were purified by Ni-NTA affinity column chromatography (Qiagen). The column was extensively washed with 200 ml of 100 mM Tris-HCl, pH 7.0 plus 500 mM NaCl, followed by a 100 ml wash with 100 mM Tris-HCl, pH 7.0, 250 mM NaCl, 30 mM imidazole followed by a final 100 ml wash with 100 mM Tris-HCl, pH 7.0, 250 mM NaCl, 45 mM imidazole. The bound E75 proteins were eluted with 25 mM Tris-HCl, pH 7.0 plus 200 mM imidazole. Pooled fractions were dialyzed in 25 mM Tris-HCl, pH 7.0, 100 mM NaCl buffer. Next, we loaded the eluted protein in a gel filtration Superdex 75 preparative grade column (GE Healthcare) equilibrated and eluted with 50 mM Tris-HCl, pH 7.0, 100 mM NaCl, in a FPLC System (Pharmacia Biotech, Uppsala, Sweden). Coloured fractions containing pure E75 were identified by SDS-PAGE. The proteins were flash frozen in liquid nitrogen.

Reduction of the heme iron and binding of CO and ·NO

In order to obtain the ferric, ferrous, ferrous-CO and ferrous-NO absorbance spectra for various insect E75 LBDs, samples (3–5 μM) were prepared under anaerobic conditions inside a glove box. Spectra were collected with protein samples (700 μl) prepared in 25 mM Tris, pH 7.0, 100 mM NaCl degassed buffer were purged of oxygen by flowing argon through the headspace of a septum-sealed vial for ~5 min. Reduction of Fe(III) protein samples using sodium dithionite was performed under an atmosphere of nitrogen using the addition of an anaerobically prepared stock solution of sodium dithionite to a final concentration of 1 mM. CO or ·NO adducts were prepared by the injection of CO(g) or ·NO(g) into the headspace of the septum-sealed cuvette via a gastight syringe followed by gentle agitation of the sample. In general, 100–200 μl of CO or ·NO gas were injected to render a complete conversion to the respective adduct. The absorption spectra at room temperature were collected on a Cary 50 Bio UV-visible spectrophotometer (Varian) until no further change was observed.

Determination of pyridine hemochromes

This assay allows the measurement of heme concentration, but also allows to determine if the prosthetic group of the protein is heme *a*, heme *b* or heme *c*. A stock pyridine solution containing 400 mM NaOH and 34% (v) pyridine was prepared in water. Then, 10 to 50 μl of concentrated protein were mixed with pyridine solution to a final volume of 500 μl in a 0.5-ml cuvette, and the oxidized spectrum was recorded between 500 and 600 nm (baseline). A few grains of solid sodium dithionite (2–5 mg) were then added and the sample was mixed by flipping the cuvette sealed with a parafilm; several successive spectra of the reduced pyridine hemochromes were recorded on a Beckman DU 640 spectrophotometer (Fullerton, CA, USA).

Circular dichroism measurements

CD spectra were recorded on a Jasco J-715 spectropolarimeter (Jasco Inc., Easton, MD, USA) using a cuvette path length of 0.1 cm and spectral collection in the range of 250–700

NIH-PA Author Manuscript

NIH-PA Author Manuscript

NIH-PA Author Manuscript

nm at 25 °C. The buffer used was 20 mM Tris, pH 8.5. A minimum of five spectra were accumulated for each sample and the contribution of the buffer was always subtracted. Raw ellipticity data were converted to mean residue ellipticity before plotting.

HPLC analysis of the heme covalent binding to protein samples

Samples were analyzed by direct injection of 100 μg of protein onto a 250 × 4.6-mm Beckman Coulter Ultrasphere C18 reversed phase column on a Beckman Coulter HPLC instrument. The protein was eluted with a linear gradient of 25–80% acetonitrile in water (0.1% trifluoroacetic acid) over 60 min (1 ml/min) with detection at 214 and 400 nm. As a control, a stock solution of hemin was prepared by dissolving 3 mg in 100 μl of 0.1 M NaOH, followed by the addition of 900 μl of water and filtrated with a filter of 0.22 μm. A 10 μl stock aliquot was diluted into 240 μl of water (0.1% trifluoroacetic acid) for analysis.

Isolation and characterization of heme-containing peptides

For the analysis of heme-containing peptides, E75B LBD from *O. fasciatus* (30 μl of a 4.5 mg/ml solution in 20 mM Tris pH 8.5) was digested with trypsin (20 μg) in 220 μl of 0.09 mM Tris pH 7.0, for 3 h at 37 °C. After this partial digestion, 50 μg of digested protein were chromatographed by direct injection onto a 250 × 4.6-mm Beckman Coulter Ultrasphere C18 reversed phase column on a Beckman Coulter HPLC instrument, with a linear gradient of 30–60% acetonitrile in water (0.1% trifluoroacetic acid) over 20 min (1 ml/min) with detection at 214 and 400 nm. A mixture of heme-containing peptides eluting at different times were collected, vacuum concentrated and analyzed by mass spectrometry. The E75B LBD from *O. fasciatus* (37.5 μl of a 4 mg/ml solution in 50 mM Tris pH 7, 100 mM NaCl) was also digested with proteinase K (18.75 μg) for 20 min at 37 °C. After this partial digestion, 50 μg of digested protein were chromatographed and analyzed as previously described.

EPR spectra

Continuous-wave (CW) EPR spectra were recorded at a low temperature (10°K) with an X-band EMX Bruker spectrometer equipped with an Oxford Instruments ESR 900 helium flow cryostat. Before being frozen, 20% (v/v) glycerol as a cryoprotectant was added to all the samples. Samples were introduced in a synthetic Suprasil quartz EPR tube and vacuum sealed before analysis.

Mass spectrometry

1 μl sample was spotted onto a MALDI target plate and allowed to air-dry at room temperature. Then, 0.5 μl of a 3 mg/ml of α-cyano-4-hydroxycinnamic acid matrix (Sigma-Aldrich) in 50% acetonitrile were added to the dried spots and allowed again to air-dry at room temperature. MALDI-TOF MS analyses were performed in a 4800 Proteomics Analyzer MALDI-TOF/TOF mass spectrometer (Applied Biosystems, MDS Sciex, Toronto, Canada) at the Genomics and Proteomics Center, Complutense University of Madrid. The MALDI-TOF/TOF operated in positive reflector mode with an accelerating voltage of 20000 V. Selected peptides, were subjected to MS/MS sequencing analyses using the 4800 Proteomics Analyzer (Applied Biosystems, Framingham, MA). Suitable precursors from the MS spectra were selected for MS/MS analyses with CID on (atmospheric gas was used) 1 Kv ion reflector mode and precursor mass Windows +/− 4 Da. The plate model & default calibration were optimized for the MS/MS spectra processing. De novo sequencing from fragmentation spectra of peptides was performed using DeNovo tool software (Applied Biosystems), tentative sequences were manually checked and validated.

NIH-PA Author Manuscript

NIH-PA Author Manuscript

NIH-PA Author Manuscript

Recombinant expression and purification of the *O. fasciatus* E75 LBD in the RP523 heme synthesis-deficient strain

The pCWori plasmid was used to transform the RP523 *E. coli* strain and expression was performed aerobically using 250 ml 2XYT cultures. When protein expression was induced by 1 mM IPTG addition, 1.25 mL of a 6 mg/ml solution of either Fe(III) protoporphyrin IX (hemin) or Fe(III) mesoporphyrin IX (mesoheme) was added to the cultures as previously described (30). Expression was performed at 25 °C and purification of the recombinant hemoproteins was performed as described above.

RESULTS

Spectral characterization of the *Drosophila melanogaster*, *Oncopeltus fasciatus* and *Bombyx mori* purified E75 LDBs

All three insect E75 LBDs were cloned in the bacterial expression system pCWori, which is suitable for recombinant heme protein expression (28). Purification of the hexa-His tagged LBDs was performed by Ni-NTA chromatography followed by gel filtration in a Superdex H75 column. The LBDs of all three E75 nuclear receptors were soluble and purified to homogeneity as hemoproteins in the absence of hemin supplementation of the cultures (Fig. S1). Whereas both the *D. melanogaster* and *B. mori* LBDs were bright red and a Soret maximum centered at 424 nm with α/β bands at 574/543 nm, the *O. fasciatus* LBD was red-brownish with a Soret displaced to 415 nm, an α band almost non-existent and a β band centered at 532 nm (Fig. 1A). Electronic absorption spectra of the *D. melanogaster* and *B. mori* insect nuclear receptor LBD constructs suggest strongly that they contain a low-spin hexacoordinate Fe(III) heme in which a histidine and a cysteine (thiolate) are present as axial ligands, in agreement with previous studies using the *D. melanogaster* isoform (3, 7, 8). In contrast, the *O. fasciatus* LBD spectrum is consistent with a myoglobin-like high-spin hexacoordinate Fe(III) heme (31) in which a histidine and (very likely) a water molecule are present as axial ligands (Fig. 1A). In addition, the *O. fasciatus* protein displayed a clear CT1 band at 655 nm which is indicative of the presence of a high-spin Fe(III) (7, 32).

Next, we compared the absorbance spectra of the three hemoproteins with their circular dichroism spectra at identical wavelengths. The δ band (porphyrin π-π* transitions) observed at 360 nm in the absorbance spectra of *D. melanogaster* and *B. mori* LBDs resulted in a positive CD band as well whereas this band was barely distinguishable from the *O. fasciatus* spectra. The γ band (Soret) observed at 424 nm in the absorbance spectra of *D. melanogaster* and *B. mori* LBDs and 415 nm in the spectrum of their *O. fasciatus* counterpart resulted in a positive CD band in all cases, although the former two proteins also display a clear negative CD band at 440 nm that is absent from the *O. fasciatus* CD spectrum (Fig. 1B). The α/β bands of the *D. melanogaster* and *B. mori* LBDs also resulted in a positive signal in their CD spectra although the *O. fasciatus* CD spectrum lacks a clear signal coming from its β band. Interestingly, the appearance of the aforementioned CT1 band at 655 nm in the *O. fasciatus* absorbance spectrum is reflected as well by a negative CD band.

Characterization of the ·NO and CO ferrous iron adducts of the three insect LBDs

The electronic absorption spectrum obtained after reduction of the heme iron of *D. melanogaster* E75 LBD with sodium dithionite exhibited a Soret maximum at 425 nm and α/β bands at 559 and 530 nm. This slight red shift upon iron reduction is also accompanied by a sharpening of the α/β bands (Fig. 2A). Binding of CO to reduced *D. melanogaster* E75 LBD results in a Soret maximum at 420 nm and α/β bands at 569 and 539 nm, consistent with a hexacoordinate heme with a His side-chain (or other neutral donor) as axial ligand (Fig. 2A). Formation of a ·NO complex (dashed line) in *D. melanogaster* E75 LBD results in

NIH-PA Author Manuscript

NIH-PA Author Manuscript

NIH-PA Author Manuscript

the appearance of a broad peak at 385 nm, consistent with a pentacoordinate NO-heme. This blue-displacement of the Soret with concomitant broadening of the α/β bands is similar to the pentacoordinate Fe(II)NO complex observed in *Rt*CooA or soluble guanylate cyclase (33, 34). Significantly, reduction of the heme iron in *O. fasciatus* E75 LBD with sodium dithionite results in a blue shift of the Soret to 425 nm accompanied by a clear sharpening of the peak as well as a better defined α/β bands at 557 and 530 nm (Fig. 2B). In analogy with its *D. melanogaster* E75 homolog, the *O. fasciatus* CO complex (dotted line) shows a sharp Soret at 420 nm, albeit the α/β bands are of a similar intensity and marginally red-shifted to 566 and 533 nm. In contrast, the ·NO adduct of ferrous *O. fasciatus* E75 LBD (dashed line) is significantly blue-shifted when compared with the *D. melanogaster* counterpart, with a Soret maximum at 416 nm and the near disappearance of the α/β bands. This spectrum is clearly reminiscent of that of the ·NO adducts observed in the case of myoglobin (35), neuroglobin (36) or *Ch*CooA (33), in which the heme is hexacoordinated with ·NO and a His residue side-chain as the iron ligands. Unexpectedly, the spectrum of the ·NO adduct of ferrous *O. fasciatus* E75 LBD, although strikingly different from the one observed for its *D. melanogaster* counterpart, is analogous to that found in its mammalian homolog Rev-erbβ (8, 13). Finally, the ferrous form of the *B. mori* E75 LBD displays a Soret maximum at 425 nm (somewhat obscured by sodium dithionite absorption) and sharp α/β bands at 559 and 530 nm (Fig. 2C). The spectra of the CO and ·NO Fe(II) complexes of the *B. mori* E75 LBD are almost indistinguishable from those of *D. melanogaster* E75 LBD, with Soret maxima at 421 and 385 nm respectively, albeit significantly different from those *O. fasciatus* E75 LBD.

EPR Spectroscopy of the insect E75 LBDs

We have also analyzed the three insect E75 LBDs in their ferric state by EPR in order to characterize and assign the heme iron axial ligands (Fig. 3). The EPR spectrum of *D. melanogaster* E75 LBD reflects heterogeneity in iron coordination, in agreement with previous data (7, 8), and contains at least two sets of rhombic signals associated with g values corresponding to low-spin ferric iron. No high-spin EPR signals were detected. All g values are within the range found for thiolate hemoproteins in which the cysteine ligand determines the EPR properties of the heme iron. A comparison of the g values with published data indicates that one component (g values: 2.54, 2.26, 1.87) corresponds to an N-donor iron ligand such as histidine and the other component (2.33, 2.26, 2.04), is compatible with O- or S-donors. The EPR spectra of *B. mori* and *D. melanogaster* E75 LBDs are very similar, although the former contains a third component with the following g values: E1 (2.54, 2.26, 1.87) and E2 (2.44, 2.26, 1.91), compatible with N- or O-donors, together with an E3 component (2.33, 2.26, 2.04). In contrast, the EPR spectrum of the *O. fasciatus* E75 LBD displays a remarkable high-spin EPR signal with a g value of 4.32 and a small high-spin EPR signal with a g value 6.02. Although the different rhombic signals are not properly defined, it can be inferred that g values are similar to those detected for the ferric form of Rev-erbβ LBD (8), the mammalian homologue of insect E75. The estimated contribution of each component to each spectrum is shown in Table 1. In addition, the tetragonal field (Δ/λ) and rhombicity (V/Δ) parameters associated with E1–E3 are also shown.

Covalent attachment of the heme moiety to the protein matrix in *O. fasciatus* E75 LBD

Next we analyzed by HPLC the elution profiles of *D. melanogaster*, *O. fasciatus* and *B. mori* E75 LBDs from a reversed phase C18 column. Elution using an acetonitrile gradient revealed that the free heme peak could be detected at ~42 min in the 400 nm channel (Fig. 4A). Whereas almost all of the *D. melanogaster* and *B. mori* heme moiety eluted as free heme with the polypeptide chain eluting at higher acetonitrile concentrations, the greater part of the *O. fasciatus* heme moiety appeared to be associated covalently with the protein (Fig. 4B, C and D). Thus, the heme moiety of *O. fasciatus* E75 LBD not only displayed

NIH-PA Author Manuscript

NIH-PA Author Manuscript

NIH-PA Author Manuscript

distinct spectroscopic properties and ·NO binding, but is also attached covalently to the protein.

Pyridine hemochrome spectra of the insect E75 LBDs

Although the formation of a pyridine hemochrome complex is a widely used method for the determination of holoprotein concentration in hemoproteins, it is also a very useful method for determining if the protein binds heme b. As expected, the pyridine hemochrome spectra of the *D. melanogaster* and *B. mori* E75 LBDs display maxima at 556 nm, characteristic of heme *b* (37) whereas formation of a pyridine hemochrome complex with the *O. fasciatus* E75 LBD gives rise to a maximum at 551 nm (Fig. 5). This complex is reminiscent of the pyridine hemochrome complex observed in the case of cytochrome *c*, a hemoprotein with heme *c* covalently bound (37).

Proteomic analysis of *Oncopeltus fasciatus* E75 LBD

Mass spectrometric analysis of proteins with heme covalently attached can sometimes reveal the amino acid side-chain involved in the linkage, at least in cases in which the proteolytic digestion does not alter the integrity of the hemopeptides. When we digested purified *Oncopeltus fasciatus* E75 LBD with trypsin and analysed the digestion products by MALDI-TOF a high coverage could be attained (Fig. S5). Unfortunately, we were unable to identify masses that could be assigned to hemopeptides with mass gains of 616 or 633 Da over the expected proteolytic trypsin products. Intriguingly, we observed peptides of 1474.88 Da and 1697.91 Da that, after fragmentation, rendered MS/MS spectra consistent with a ^{240}FLMDSMFDFAER^{251} sequence in which Met245 had lost 34 Da or gained 189 Da, respectively (Fig. S6). These results led to the conclusion that the heme moiety might be attached to the polypeptide chain of the *O. fasciatus* E75 LBD through a methionine vinyl-sulfonium bond in analogy with that observed in the case of myeloperoxidase (23, 38) or perhaps through a methionine ethyl-sulfonium as in the Ser160Met mutant of ascorbate peroxidase (39). Hence, fragmentation of the Met245 side-chain after trypsin hydrolysis rendered a peptide ^{240}FLMDSMFDFAER^{251} with a 34 Da mass loss. Likewise peptide ^{240}FLMDSMFDFAER^{251} with a mass gain of 189 Da in Met245 very likely arises from a fragmented heme adduct that remains attached to the amino acid side-chain. Since no atomic information is available in the case of insect E75 LBDs, we inspected the position of Met486 in the recently obtained crystal structure of its mammalian homologue Rev-erbβ (13). As shown in Fig. S7, Met486 in Rev-erbβ would be the equivalent to *O. fasciatus* Met245 (Fig. S2) and both would be positioned in helix 7 with the sulphur atom in close proximity to one of the heme vinyl groups, hence reinforcing the mass spectrometric data indicating that the side-chain of Met245 might be involved in one of the covalent bonds with the heme moiety. Support for attachment of the heme group to Met245 in *O. fasciatus* E75 LBD was obtained by the fact that both the *D. melanogaster* and *B. mori* proteins have a Thr residue at the equivalent position in helix 7 (Fig. S2).

In addition to trypsin, partial digestion of the purified *O. fasciatus* E75 LBD with other proteases, including pronase or proteinase K, followed by HPLC analysis also revealed the presence of hemopeptides (Fig. S8). Unfortunately, our MS/MS analysis failed to unambiguously identity additional linkages between the heme and protein moiety.

Recombinant expression and purification of *O. fasciatus* E75 LBD in the RP523 heme synthesis-deficient *E. coli* strain

The intriguing possibility that the heme vinyl groups are involved in the covalent attachment to an amino acid side-chain was next explored using an *E. coli* strain defective in heme synthesis. Addition of porphyrin analogs to the bacterial medium permits the purification of heme-substituted hemoproteins that can be subsequently compared to their wild-type Fe-

NIH-PA Author Manuscript

NIH-PA Author Manuscript

NIH-PA Author Manuscript

protoporphyrin IX counterparts (30, 40). With that in mind, we grew RP523 *E. coli* transformed with wild-type *O. fasciatus* E75 LBD in the presence of Fe(III) mesoheme, a heme derivative in which the vinyl groups have been substituted with ethyl groups. In a parallel experiment, wild-type *O. fasciatus* E75 LBD was also expressed in RP523 *E. coli* supplemented with Fe(III) protoporphyrin IX (hemin). Purification of Fe(III) protoporphyrin IX-bound *O. fasciatus* E75 LBD in RP523 *E. coli* cells revealed that the prosthetic group was successfully incorporated and, as expected, the Soret maximum was centered at 413 nm (Fig. 6A). In addition, the position of the α/β bands and the CT1 band also is undistinguishable from that shown in the *O. fasciatus* spectrum shown above (Fig. 1A). On the other hand, the mesoheme-saturated *O. fasciatus* E75 LBD revealed a sharp blue-shifted Soret maximum at 406 nm, a complete absence of CT1 band and diminished heme incorporation (approximately 69% when compared with its Fe(III) protoporphyrin IX-bound counterpart). HPLC analysis of these two purified recombinant proteins revealed that 51% of the heme in *O. fasciatus* E75 LBD expressed in RP523 *E. coli* supplemented with Fe(III) protoporphyrin IX remained covalently attached to the protein polypeptide chain (Fig. 6B, upper panel). This in is clear contrast with the *O. fasciatus* E75 LBD expressed in RP523 *E. coli* supplemented with Fe(III) mesoporphyrin IX, in which the heme group is completely unable to bind covalently to the protein moiety with 100% of the heme absorbance eluting earlier than the polypeptide chain (Fig. 6B, bottom panel). The position of this peak is consistent with the elution profile of free Fe(III) mesoporphyrin IX, that shows a sharp peak at 45 minutes (data not shown). These results strongly support the conclusion that covalent heme binding naturally occurs and clearly establishes that the vinyl groups are the site of covalent binding.

Characterization of *Dros/Onc* and *Onc/Dros* protein chimeras

Due to the high sequence similarity at the amino acid level among the three insect E75 LBDs (Fig. S2) we concluded that very few residues present in the *O. fasciatus* isoform could be responsible for its different spectroscopic properties and also for the heme to protein covalent attachment. In addition, we wondered if these two phenotypes were connected. With that in mind we designed *D. melanogaster/O. fasciatus* and *O. fasciatus/D. melanogaster* chimeric E75 LBDs (Fig. S3). Since residues in helix 5 are extremely similar among the various E75 proteins, the conserved TLLKAG amino acid motif, identical in both *D. melanogaster* and *O. fasciatus* was selected as the connection part between the sequences. The absorption spectra of the Fe(III) forms of both the *Dros/Onc* and the *Onc/Dros* chimeras are shown in Fig. 7A. Intriguingly, in both cases the Soret (γ band) shows a peak at 422 nm, which is closer to the wild-type *D. melanogaster* E75 LBD (maximum at 424 nm) than to wild-type *O. fasciatus* E75 LBD (415 nm). However, the *Onc/Dros* chimera displayed a clear β band at 537 nm together with a small α band at 574 nm, followed by a clear CT1 band at 655 nm whereas the *Dros/Onc* chimera displayed a clear β band at 543 nm together with a small α band at 574 nm, followed by a faint but discernible CT1 band at 655 nm. Hence, these absorbance spectra share components from both wild-type *O. fasciatus* and *D. melanogaster* spectra although the CT1 band at 655 nm seems to arise from the interaction of the heme moiety with residues located in the N-terminal part of the *O. fasciatus* E75 LBD. The Fe(III) form of wild-type *D. melanogaster* E75 LBD displayed α/β bands at 574 and 543 nm, respectively, both being present in the chimeric constructs, albeit with a slightly blue-shifted β band. On the other hand, the Fe(III) form of wild-type *O. fasciatus* E75 LBD displayed a clear β band at 532 nm together with a CT1 band at 655 nm, this high spin component being clearly visible in the Onc/Dros chimera and to a lesser extent in the *Dros/Onc* chimera (Fig. S4). HPLC analysis of the *Onc/Dros* and *Dros/Onc* chimeras revealed that, in both cases, a significant amount of heme remained attached to the protein moiety (Fig. 7B). This suggests that a heme to protein covalent bond is retained in each of the chimeras and strongly supports the hypothesis that heme is attached to the wild-type *O.*

NIH-PA Author Manuscript

NIH-PA Author Manuscript

NIH-PA Author Manuscript

fasciatus E75 LBD through at least two covalent bonds, one positioned at the N-terminus half of the polypeptide chain and the other at its C-terminal half. Quantitation of the ratio of free to bound heme in the various hemoproteins revealed that both of the chimeras partially bind heme covalently although to a lesser extent than the wild-type *O. fasciatus* E75 LBD (Table 2).

Characterization of the *O. fasciatus* Glu158Lys and Met245Thr mutants

Spectroscopic characterization of the Met245Thr *O. fasciatus* E75 LBD mutant protein revealed a Soret maximum centered at 413 nm, an almost non-existing α band and a β band centered at 532 nm. Furthermore, the Met245Thr *O. fasciatus* E75 LBD mutant protein displayed a clear CT1 band at 655 nm (Fig. 8A), in agreement with the previous observation that the appearance of this band is the result of the interaction of the heme with residues located at the N-terminus of *O. fasciatus* E75 LBD. HPLC analysis of this mutant protein showed that approximately 18% of the total heme eluted as free heme, twice as much as the amount found in the wild-type protein (Table 2). Thus, elimination of Met245 did not introduce major changes in the spectroscopic properties of the hemoprotein when compared with the wild-type counterpart, although the mutation modestly increased the amount of heme that was not covalently linked to the protein moiety. Our data specifically suggest that at least two amino acid side-chains are responsible for the covalent linkage to the heme group and that the spectroscopic properties of the *O. fasciatus* E75 LBD are mostly determined by the proximal and distal iron ligands as well as by other amino acids present in the environment of the heme rather that by the covalent linkage to the protein backbone.

In addition to a covalent vinyl sulfonium bridge between a heme vinyl group and a Met residues such as that in myeloperoxidase, other proteins such as cytochromes P450 of the CYP4A family bind heme through the side-chain of Glu residues (20). Hence, we also created a Glu158Lys mutant, as this amino acid, present in *O. fasciatus* but absent in *D. melanogaster* and *B. mori* E75 LBD isoforms (Fig. S2) is predicted to be positioned at the N-terminus of helix 3 in proximity of the heme group (Fig. S7). Nonetheless, both the spectral properties and HPLC elution profile of *O. fasciatus* Glu158Lys mutant were virtually indistinguishable from those of its wild-type counterpart (Fig. 8B).

Recombinant expression and purification of *Blattella germanica* E75 LBD

Next we wondered if the spectral properties and covalent linkage of the heme group to the protein were a particular characteristic of the *O. fasciatus* E75 LBD, or if they were shared by other insect E75 nuclear receptors. Sequence comparison showed that the homologous E75 LBD of the German cockroach (*Blattella germanica*) displayed a large degree of sequence identity with its *O. fasciatus* counterpart (Fig. S2). Thus, we cloned, expressed in bacteria and purified the E75 LBD of *B. germanica* (residues 148–402). As expected, the recombinant protein was purified as a hemoprotein in its ferric form with a brownish colour that highly resembled that of the *O. fasciatus* E75 LBD (data not shown). The Soret maximum was centered at 415 nm, the α band was almost non-existent, the β band was centered at 533 nm and a CT1 band appeared at 655 nm (Fig. 9A). These spectroscopic properties of the *B. germanica* E75 LBD were clearly different from those of the *D. melanogaster* and *B. mori* E75 LBDs and almost identical to those shown by the *O. fasciatus* E75 LBD (Fig. 1A). HPLC analysis (Fig. 9B) showed that the majority of the heme remained bound to the protein moiety in the *B. germanica* E75 LBD (Table 2), in agreement with the behaviour displayed by its *O. fasciatus* counterpart. These results led to the conclusion that the LBDs of certain E75 nuclear receptors bind the heme group covalently.

NIH-PA Author Manuscript

NIH-PA Author Manuscript

NIH-PA Author Manuscript

Discussion

In metazoans, nuclear receptors have been classically defined as ligand activated transcription factors that allow the regulation of target genes by small lipophilic molecules such as hormones (steroids, thyroid hormones), morphogens (retinoic acid) and dietary components (fatty acids) (41, 42). Most of the nuclear receptors have distinctive modular domains designated (from the N-terminus) as A/B, C, D, E and F (42, 43). The C domain consists of the DNA-binding domain and possesses invariant Cys residues that stabilize several zinc fingers. The E domain consists of the LBD which permits nuclear receptors to function as ligand-dependent transcriptional regulators. The genome of the insect *D. melanogaster* encodes only 18 nuclear receptors with both a functional DNA binding domain and a LBD (44). In spite of being an extensively studied organism, many *D. melanogaster* nuclear receptors remain orphan, still awaiting the identification of endogenous or xenobiotic ligands. Remarkably, recent studies have shown that heme is present in the orphan nuclear receptor E75 purified from insects (3) and that heme appears associated to the E75 LBD when purified from a heterologous expression system (3, 7, 8). Soon after, two groups independently found that Rev-erbα and Rev-erbβ, the human homologs of *D. melanogaster* E75, also bind heme (11–13). Heme binding to these nuclear receptors can be explained assuming that they might function, perhaps even simultaneously, as sensors of cellular heme levels, redox changes or concentrations of diatomic gases, subsequently regulating the expression of a variety of genes.

Indeed, it has been suggested that *D. melanogaster* E75 might use heme as a ligand, hence functioning as a heme sensor (3, 8), a suggestion reinforced by the observation that heme bound to E75 at a 1:1 stoichiometry, enhanced the thermal stability of the protein and was required for proper folding and functioning of the E75 (3). Nevertheless, a caveat exists to the conclusion that heme binds and is released from E75, as a true ligand would be, since the LBD of E75 is always purified heme-saturated in bacterial expression systems (3, 7, 8) and 5 M guanidine hydrochloride is unable to release the heme moiety from purified E75 (3). We have also observed that a significant amount of heme remains bound to purified *D. melanogaster* E75 LBD in SDS-PAGE (data not shown). In contrast, Rev-erbα and Rev-erbβ, the mammalian homologs of insect E75 LBD, seem to be bona fide heme sensors since both proteins can be purified in the absence of heme (13, 45), isothermal titration calorimetry can be used to determine the heme binding constant for both apoRev-erbα and apoRev-erbβ (12), and atomic crystallographic data is available for both apo and heme-bound Rev-erbα (45) and Rev-erbβ (13, 46). In addition, heme binding promotes recruitment of nuclear co-repressor and histone deacetylase (12, 13, 47), with Rev-erbα recruiting HDAC3 and Rev-erbβ recruiting HDAC1 (15). Finally, whereas wild-type Rev-erbβ can repress transcription of target genes, its His602Phe mutant, which is unable to bind heme, does not display this transcriptional repressor activity in cotransfection assays (12).

Secondly, *D. melanogaster* E75 can detect changes in redox condition in the sense that Fe(II), but not Fe(III) E75 LBD, can bind to a peptide derived from its HR3 partner, hence suggesting that heteroassociation and repression of transcription occurs when the iron group is in its reduced form (3, 8).

Finally, the interaction of *D. melanogaster* E75 LBD with diatomic gases is well documented both in vivo and in vitro, although only ·NO binding to E75 LBD has been observed and characterized in vivo (3, 5–8). Binding of both CO and ·NO to the ferrous heme group of purified *D. melanogaster* E75 blocked its ability to bind to a peptide derived from HR3 (3). In transfection assays HR3 on its own acts as a transcriptional activator, albeit in the presence of transfected E75, its activity becomes significantly reduced. The addition of an ·NO donor, such as DETA-NO, to the cotransfected cells results in the

NIH-PA Author Manuscript

NIH-PA Author Manuscript

NIH-PA Author Manuscript

formation of a heme-NO complex in E75, interferes with its association to HR3 and results in the rescue of its transcriptional activity (3). In vivo, ·NO release by *D. melanogaster* NOS in the prothoracic gland blocks the ability of E75 to interfere with HR3-mediated transcriptional activation (5). Chromatin immunoprecipitation also revealed that ·NO inhibits the recruitment of the co-repressor SMRTER by E75 (6).

In this manuscript we have characterized and compared the heme coordination of constructs of the E75 LBD hemoproteins from four different insects: *Drosophila melanogaster*, *Bombyx mori*, *Oncopeltus fasciatus* and *Blattella germanica*. Whereas *B. mori* E75 LBD is spectroscopically similar to its *D. melanogaster* counterpart, both the *O. fasciatus* and the *B. germanica* E75 LBD are purified as high-spin hemoproteins with the heme moiety covalently attached to the side-chains of at least two amino acid residues. In addition, our EPR data indicate that *O. fasciatus* E75 LBD is purified with a mixture of high and low spin components. Although no atomic resolution structure of insect E75 LBD is available, the crystal structure of a tryptic fragment of Rev-erbβ with heme bound indicate that Rev-erbβ Cys384 and His566 are the axial ligands for the heme group. Moreover, in light of the crystal structure of heme-bound Rev-erbβ several residues positioned in the N-terminus of helix 3 have been proposed as surrogate heme axial ligands upon conformational changes (13). It must be noted that the equivalent residues to Rev-erbβ Cys384 and His566 are conserved in *D. melanogaster* (Cys396, His574), *B. mori* (Cys193, His371), *O. fasciatus* (Cys144, His327) and *B. germanica* (Cys204, His387) E75 LBDs (Fig. S2). Nevertheless, site directed mutagenesis has revealed that in *D. melanogaster* Cys368, Cys385 and Cys468 are also markedly involved in heme binding (7). Sequence inspection reveals that both *O. fasciatus* and *B. germanica* E75 LBDs display an amino acid extension of the N-terminus of helix 3 that is absent from the *D. melanogaster* and *B. mori* E75 LBD isoforms. This part of the nuclear receptor is predicted to be positioned closed to the heme group and is likely to establish one of the covalent linkages to the heme moiety (Fig. S7). Our results indicate that *O. fasciatus* Met245 would also be covalently bound to the heme group. The absence of major spectroscopic changes in our Met245Thr mutant probably reflects the reduction of the heme vinyl group and the formation of an ethyl linkage between protein and heme moieties. This would be analogous to linkage found in cyanobacterial hemoglobins (48, 49) and in ascorbate peroxidase Ser160Met mutant (39) and different from the vinyl sulfonium linkage of myeloperoxidase (23, 38). Furthermore, strong evidence in favour of the heme vinyl groups as key elements in the covalent linkage is provided by the absence of attachment of mesoheme to the protein moiety of *O. fasciatus* E75 LBD when expressed in the RP523 *E. coli* strain. Sequence inspection reveals that very few residues present in the *O. fasciatus* and *B. germanica* isoforms could be responsible for their unique spectroscopic properties and their heme to protein covalent attachment. The results obtained using our *Drosophila/Oncopeltus* chimeric hemoproteins reveal that a heme attachment site must be present N-terminal and another one C-terminal of helix 3.

Our data also strongly suggest that insect E75 LBDs are very unlikely to function as heme sensors in vivo, since covalently-linked heme cannot be released from the hydrophobic pocket of the protein. In this regard, it must be noted that the tight heme binding previously reported for *D. melanogaster* E75 LBD and the impossibility to purify heme-free protein indicate that the binding and release of heme is also unlikely to occur in these species. It is not fully understood why heme becomes covalently bound in some proteins or even only in some members of a protein family. For example only a few members of the CYP4 family of cytochrome P450 covalently bind their heme, so covalent heme attachment satisfies a requirement that is specific for some of them. Covalent binding of the heme to the protein may allow a finer discrimination against exposure of the (ϖ-1)-methylene group to the ferryl species and thus enhance the ϖ-regiospecificity of the enzyme (20).

NIH-PA Author Manuscript

NIH-PA Author Manuscript

NIH-PA Author Manuscript

Our data do support the role of insect E75 LBDs as diatomic gas sensors. Notwithstanding being aerobically purified as ferric hemoproteins, in order to become regulated through ·NO and CO binding in vivo it is tempting to speculate that insect E75 LBDs should be present in their ferrous form in the cell nucleus. The Fe(II) absorbance spectra of all *D. melanogaster*, *O. fasciatus* and *B. mori* E75 LBDs are very similar (Fig. 2), with Soret maximum at 425 nm and sharp α/β bands at 559 and 530 nm, indicative of replacement or loss of the cysteine (thiolate) ligand, in agreement with previous data (8). Significantly, anaerobic titration revealed that the ferrous form of *O. fasciatus* E75 LBD readily formed both ·NO and CO complexes, implying that in vivo diatomic gases very likely regulate its transcription repression activity as well. In accordance with the proposed models (3, 7, 8), this conformational change induced by ·NO or CO binding should eventually also result in the release of *O. fasciatus* HR3 partner. However, the published spectra of the ·NO adducts of purified E75 and Rev-erbβ LBDs are markedly different (8). Whereas the ·NO complex of both *D. melanogaster* and *B. mori* E75 LBDs, with a maximum at 385 nm, are characteristic of a 5-coordinate hemoprotein, those of Rev-erbβ LBD (with an absorbance maximum at 418 nm) and *O. fasciatus* E75 LBD (with an absorbance maximum at 416 nm), correspond very likely to a 6-coordinate heme with the side-chain of a His residue *trans* to ·NO (3, 7, 8). Similarly, 6-coordinate Fe(II)NO complexes have been described for myoglobin (Soret at 421 nm (35)), horseradish peroxidase (Soret at 419 nm (50)), neuroglobin (Soret at 416 nm (36)) or *Ch*CooA (Soret at 418 nm (51)).

It is unclear what advantage is provided by covalent binding of the heme in these two members, given that the heme is fully functional in the non-covalently bound state in *D. melanogaster* and *B. mori* E75 LBDs. The fact that covalently bound heme in *O. fasciatus* E75 LBD readily responds to the presence of CO and ·NO indicates that diatomic gases are also involved in signalling through this nuclear receptor, although its downstream effector biomolecules might be different. I nterestingly major differences have been recently discovered regarding the temporary expression pattern and the parasegment specification of the E75 gene between *D. melanogaster* and *O. fasciatus*. First of all, unlike E75A in *D. melanogaster*, the *O. fasciatus* E75A gene is a pair-rule gene required for specification of odd-numbered parasegments (26). Whereas in *D. melanogaster* E75A the mRNA is maternally inherited, evenly distributed and first transcribed between 6 and 8 h after egg deposition (52), the pair-rule genes, such as that of *O. fasciatus* E75A are expressed between 1.5 and 3 h, from the onset of cellularization through gastrulation (26). Strong evidence in favour of a different signalling pathway between *D. melanogaster* and its *O. fasciatus* and *B. germanica* homologs is provided by the observation that E75A expression in postembryonic development is initiated by ecdysteroid, and the appearance of the different isoforms depends on the changing ecdysteroid titer (52, 53). Conversely, whether ecdysteroids might be responsible for initiating E75 expression in *O. fasciatus* and *B. germanica* embryos is unclear. Furthermore, E75A mRNA was found in the early embryo of *B. germanica*, but was not correlated with an increase in ecdysteroid titer (27). Our results indicate that although all four insect E75 LBDs characterized in this work are purified as hemoproteins, the covalent heme attachment might serve different functions in vivo. The possibility therefore exists that different insect species regulate signalling through E75 nuclear receptors in divergent ways.

Supplementary Material

Refer to Web version on PubMed Central for supplementary material.

Acknowledgments

We are grateful to Felipe Clemente from the Proteomics unit at the Complutense University and Sara Abián for help with the HPLC. We are also indebted to Javier Merino Gracia for help with the PyMol figure. We thank

Hugues Ouellet for assistance with the gas binding studies and Fatbardha Varfaj for help with the initial heme binding studies. This work was funded with Spanish grant BFU2009-10442 and NIH grants AI074824 and GM25515.

Abbreviations used

Bmal1	Brain, muscle Arnt-like protein-1
CD	circular dichroism
***Ch*CooA**	CO activator protein from *Carboxydothermus hydrogenoformans*
CO	carbon monoxide
DETA-NO	diethylenetriamine NONOate
E75	ecdysone-induced protein 75
EPR	electron paramagnetic resonance
HDAC	histone deacetylase
HO	heme oxygenase
HPLC	high pressure liquid chromatography
HR3	hormone receptor 3
LBD	ligand binding domain
NCoR	nuclear receptor co-repressor
·NO	nitric oxide
NOS	nitric oxide synthase
***Rr*CooA**	CO activator protein from *Rhodospirillum rubrum*
SMRT	silencing mediator for retinoid and thyroid hormone receptor
SMRTER	NCoR/SMRT-related molecule in *Drosophila*

References

1. Hiruma K, Riddiford LM. Differential control of MHR3 promoter activity by isoforms of the ecdysone receptor and inhibitory effects of E75A and MHR3. Dev Biol. 2004; 272:510–521. [PubMed: 15282165]
2. White KP, Hurban P, Watanabe T, Hogness DS. Coordination of Drosophila metamorphosis by two ecdysone-induced nuclear receptors. Science. 1997; 276:114–117. [PubMed: 9082981]
3. Reinking J, Lam MM, Pardee K, Sampson HM, Liu S, Yang P, Williams S, White W, Lajoie G, Edwards A, Krause HM. The Drosophila nuclear receptor e75 contains heme and is gas responsive. Cell. 2005; 122:195–207. [PubMed: 16051145]
4. Swevers L, Ito K, Iatrou K. The BmE75 nuclear receptors function as dominant repressors of the nuclear receptor BmHR3A. J Biol Chem. 2002; 277:41637–41644. [PubMed: 12200421]
5. Caceres L, Necakov AS, Schwartz C, Kimber S, Roberts IJ, Krause HM. Nitric oxide coordinates metabolism, growth, and development via the nuclear receptor E75. Genes Dev. 2011; 25:1476–1485. [PubMed: 21715559]
6. Johnston DM, Sedkov Y, Petruk S, Riley KM, Fujioka M, Jaynes JB, Mazo A. Ecdysone- and NO-mediated gene regulation by competing EcR/Usp and E75A nuclear receptors during Drosophila development. Mol Cell. 2011; 44:51–61. [PubMed: 21981918]
7. de Rosny E, de Groot A, Jullian-Binard C, Gaillard J, Borel F, Pebay-Peyroula E, Fontecilla-Camps JC, Jouve HM. Drosophila nuclear receptor E75 is a thiolate hemoprotein. Biochemistry. 2006; 45:9727–9734. [PubMed: 16893174]

NIH-PA Author Manuscript NIH-PA Author Manuscript NIH-PA Author Manuscript

NIH-PA Author Manuscript

NIH-PA Author Manuscript

NIH-PA Author Manuscript

8. Marvin KA, Reinking JL, Lee AJ, Pardee K, Krause HM, Burstyn JN. Nuclear receptors homo sapiens Rev-erbbeta and Drosophila melanogaster E75 are thiolate-ligated heme proteins which undergo redox-mediated ligand switching and bind CO and NO. Biochemistry. 2009; 48:7056–7071. [PubMed: 19405475]
9. Harding HP, Lazar MA. The monomer-binding orphan receptor Rev-Erb represses transcription as a dimer on a novel direct repeat. Mol Cell Biol. 1995; 15:4791–4802. [PubMed: 7651396]
10. Duez H, Staels B. Rev-erb alpha gives a time cue to metabolism. FEBS Lett. 2008; 582:19–25. [PubMed: 17765229]
11. Yin L, Wu N, Curtin JC, Qatanani M, Szwergold NR, Reid RA, Waitt GM, Parks DJ, Pearce KH, Wisely GB, Lazar MA. Rev-erbalpha, a heme sensor that coordinates metabolic and circadian pathways. Science. 2007; 318:1786–1789. [PubMed: 18006707]
12. Raghuram S, Stayrook KR, Huang P, Rogers PM, Nosie AK, McClure DB, Burris LL, Khorasanizadeh S, Burris TP, Rastinejad F. Identification of heme as the ligand for the orphan nuclear receptors REV-ERBalpha and REV-ERBbeta. Nat Struct Mol Biol. 2007; 14:1207–1213. [PubMed: 18037887]
13. Pardee KI, Xu X, Reinking J, Schuetz A, Dong A, Liu S, Zhang R, Tiefenbach J, Lajoie G, Plotnikov AN, Botchkarev A, Krause HM, Edwards A. The structural basis of gas-responsive transcription by the human nuclear hormone receptor REV-ERBbeta. PLoS Biol. 2009; 7:e43. [PubMed: 19243223]
14. Ramakrishnan SN, Muscat GE. The orphan Rev-erb nuclear receptors: a link between metabolism, circadian rhythm and inflammation? Nucl Recept Signal. 2006; 4:e009. [PubMed: 16741567]
15. Gupta N, Ragsdale SW. Thiol-disulfide redox dependence of heme binding and heme ligand switching in nuclear hormone receptor rev-erb{beta}. J Biol Chem. 2011; 286:4392–4403. [PubMed: 21123168]
16. Bushnell GW, Louie GV, Brayer GD. High-resolution three-dimensional structure of horse heart cytochrome c. J Mol Biol. 1990; 214:585–595. [PubMed: 2166170]
17. LeBrun LA, Xu F, Kroetz DL, Ortiz de Montellano PR. Covalent attachment of the heme prosthetic group in the CYP4F cytochrome P450 family. Biochemistry. 2002; 41:5931–5937. [PubMed: 11980497]
18. LeBrun LA, Hoch U, Ortiz de Montellano PR. Autocatalytic mechanism and consequences of covalent heme attachment in the cytochrome P4504A family. J Biol Chem. 2002; 277:12755–12761. [PubMed: 11821421]
19. Zheng YM, Baer BR, Kneller MB, Henne KR, Kunze KL, Rettie AE. Covalent heme binding to CYP4B1 via Glu310 and a carbocation porphyrin intermediate. Biochemistry. 2003; 42:4601–4606. [PubMed: 12693958]
20. Colas C, Ortiz de Montellano PR. Autocatalytic radical reactions in physiological prosthetic heme modification. Chem Rev. 2003; 103:2305–2332. [PubMed: 12797831]
21. Henne KR, Kunze KL, Zheng YM, Christmas P, Soberman RJ, Rettie AE. Covalent linkage of prosthetic heme to CYP4 family P450 enzymes. Biochemistry. 2001; 40:12925–12931. [PubMed: 11669629]
22. Colas C, Kuo JM, Ortiz de Montellano PR. Asp-225 and glu-375 in autocatalytic attachment of the prosthetic heme group of lactoperoxidase. J Biol Chem. 2002; 277:7191–7200. [PubMed: 11756449]
23. Fiedler TJ, Davey CA, Fenna RE. X-ray crystal structure and characterization of halide-binding sites of human myeloperoxidase at 1.8 A resolution. J Biol Chem. 2000; 275:11964–11971. [PubMed: 10766826]
24. Pipirou Z, Bottrill AR, Metcalfe CM, Mistry SC, Badyal SK, Rawlings BJ, Raven EL. Autocatalytic formation of a covalent link between tryptophan 41 and the heme in ascorbate peroxidase. Biochemistry. 2007; 46:2174–2180. [PubMed: 17263562]
25. Pipirou Z, Guallar V, Basran J, Metcalfe CL, Murphy EJ, Bottrill AR, Mistry SC, Raven EL. Peroxide-dependent formation of a covalent link between Trp51 and the heme in cytochrome c peroxidase. Biochemistry. 2009; 48:3593–3599. [PubMed: 19249872]

NIH-PA Author Manuscript

NIH-PA Author Manuscript

NIH-PA Author Manuscript

26. Erezyilmaz DF, Kelstrup HC, Riddiford LM. The nuclear receptor E75A has a novel pair-rule-like function in patterning the milkweed bug, Oncopeltus fasciatus. Dev Biol. 2009; 334:300–310. [PubMed: 19580803]
27. Mane-Padros D, Cruz J, Vilaplana L, Pascual N, Belles X, Martin D. The nuclear hormone receptor BgE75 links molting and developmental progression in the direct-developing insect Blattella germanica. Dev Biol. 2008; 315:147–160. [PubMed: 18207139]
28. Rodriguez-Crespo I, Ortiz de Montellano PR. Human endothelial nitric oxide synthase: expression in Escherichia coli, coexpression with calmodulin, and characterization. Arch Biochem Biophys. 1996; 336:151–156. [PubMed: 8951046]
29. Rodriguez-Crespo I, Nishida CR, Knudsen GM, de Montellano PR. Mutation of the five conserved histidines in the endothelial nitric-oxide synthase hemoprotein domain. No evidence for a non-heme metal requirement for catalysis. J Biol Chem. 1999; 274:21617–21624. [PubMed: 10419469]
30. Woodward JJ, Martin NI, Marletta MA. An Escherichia coli expression-based method for heme substitution. Nat Methods. 2007; 4:43–45. [PubMed: 17187078]
31. Gonzalez G, Dioum EM, Bertolucci CM, Tomita T, Ikeda-Saito M, Cheesman MR, Watmough NJ, Gilles-Gonzalez MA. Nature of the displaceable heme-axial residue in the EcDos protein, a heme-based sensor from Escherichia coli. Biochemistry. 2002; 41:8414–8421. [PubMed: 12081490]
32. Neri F, Indiani C, Baldi B, Vind J, Welinder KG, Smulevich G. Role of the distal phenylalanine 54 on the structure, stability, and ligand binding of Coprinus cinereus peroxidase. Biochemistry. 1999; 38:7819–7827. [PubMed: 10387022]
33. Reynolds MF, Parks RB, Burstyn JN, Shelver D, Thorsteinsson MV, Kerby RL, Roberts GP, Vogel KM, Spiro TG. Electronic absorption, EPR, and resonance raman spectroscopy of CooA, a CO-sensing transcription activator from R. rubrum, reveals a five-coordinate NO-heme. Biochemistry. 2000; 39:388–396. [PubMed: 10631000]
34. Stone JR, Sands RH, Dunham WR, Marletta MA. Electron paramagnetic resonance spectral evidence for the formation of a pentacoordinate nitrosyl-heme complex on soluble guanylate cyclase. Biochem Biophys Res Commun. 1995; 207:572–577. [PubMed: 7864845]
35. Decatur SM, Franzen S, DePillis GD, Dyer RB, Woodruff WH, Boxer SG. Trans effects in nitric oxide binding to myoglobin cavity mutant H93G. Biochemistry. 1996; 35:4939–4944. [PubMed: 8664286]
36. Herold S, Fago A, Weber RE, Dewilde S, Moens L. Reactivity studies of the Fe(III) and Fe(II)NO forms of human neuroglobin reveal a potential role against oxidative stress. J Biol Chem. 2004; 279:22841–22847. [PubMed: 15020597]
37. Berry EA, Trumpower BL. Simultaneous determination of hemes a, b, and c from pyridine hemochrome spectra. Anal Biochem. 1987; 161:1–15. [PubMed: 3578775]
38. Kooter IM, Moguilevsky N, Bollen A, van der Veen LA, Otto C, Dekker HL, Wever R. The sulfonium ion linkage in myeloperoxidase. Direct spectroscopic detection by isotopic labeling and effect of mutation. J Biol Chem. 1999; 274:26794–26802. [PubMed: 10480885]
39. Metcalfe CL, Ott M, Patel N, Singh K, Mistry SC, Goff HM, Raven EL. Autocatalytic formation of green heme: evidence for H2O2-dependent formation of a covalent methionine-heme linkage in ascorbate peroxidase. J Am Chem Soc. 2004; 126:16242–16248. [PubMed: 15584761]
40. Tejero J, Biswas A, Haque MM, Wang ZQ, Hemann C, Varnado CL, Novince Z, Hille R, Goodwin DC, Stuehr DJ. Mesohaem substitution reveals how haem electronic properties can influence the kinetic and catalytic parameters of neuronal NO synthase. Biochem J. 2011; 433:163–174. [PubMed: 20950274]
41. Markov GV, Laudet V. Origin and evolution of the ligand-binding ability of nuclear receptors. Mol Cell Endocrinol. 2011; 334:21–30. [PubMed: 21055443]
42. Fahrbach SE, Smagghe G, Velarde RA. Insect nuclear receptors. Annu Rev Entomol. 2012; 57:83–106. [PubMed: 22017307]
43. Escriva H, Bertrand S, Laudet V. The evolution of the nuclear receptor superfamily. Essays Biochem. 2004; 40:11–26. [PubMed: 15242336]
44. King-Jones K, Thummel CS. Nuclear receptors--a perspective from Drosophila. Nat Rev Genet. 2005; 6:311–323. [PubMed: 15803199]

NIH-PA Author Manuscript

NIH-PA Author Manuscript

NIH-PA Author Manuscript

45. Phelan CA, Gampe RT Jr, Lambert MH, Parks DJ, Montana V, Bynum J, Broderick TM, Hu X, Williams SP, Nolte RT, Lazar MA. Structure of Rev-erbalpha bound to N-CoR reveals a unique mechanism of nuclear receptor-co-repressor interaction. Nat Struct Mol Biol. 2010; 17:808–814. [PubMed: 20581824]

46. Woo EJ, Jeong DG, Lim MY, Jun Kim S, Kim KJ, Yoon SM, Park BC, Ryu SE. Structural insight into the constitutive repression function of the nuclear receptor Rev-erbbeta. J Mol Biol. 2007; 373:735–744. [PubMed: 17870090]

47. Yin L, Lazar MA. The orphan nuclear receptor Rev-erbalpha recruits the N-CoR/histone deacetylase 3 corepressor to regulate the circadian Bmal1 gene. Mol Endocrinol. 2005; 19:1452–1459. [PubMed: 15761026]

48. Vu BC, Nothnagel HJ, Vuletich DA, Falzone CJ, Lecomte JT. Cyanide binding to hexacoordinate cyanobacterial hemoglobins: hydrogen-bonding network and heme pocket rearrangement in ferric H117A Synechocystis hemoglobin. Biochemistry. 2004; 43:12622–12633. [PubMed: 15449952]

49. Vu BC, Vuletich DA, Kuriakose SA, Falzone CJ, Lecomte JT. Characterization of the heme-histidine cross-link in cyanobacterial hemoglobins from Synechocystis sp. PCC 6803 and Synechococcus sp. PCC 7002. J Biol Inorg Chem. 2004; 9:183–194. [PubMed: 14727166]

50. Ischiropoulos H, Nelson J, Duran D, Al-Mehdi A. Reactions of nitric oxide and peroxynitrite with organic molecules and ferrihorseradish peroxidase: interference with the determination of hydrogen peroxide. Free Radic Biol Med. 1996; 20:373–381. [PubMed: 8720908]

51. Clark RW, Lanz ND, Lee AJ, Kerby RL, Roberts GP, Burstyn JN. Unexpected NO-dependent DNA binding by the CooA homolog from Carboxydothermus hydrogenoformans. Proc Natl Acad Sci U S A. 2006; 103:891–896. [PubMed: 16410360]

52. Dubrovsky EB, Dubrovskaya VA, Berger EM. Hormonal regulation and functional role of Drosophila E75A orphan nuclear receptor in the juvenile hormone signaling pathway. Dev Biol. 2004; 268:258–270. [PubMed: 15063166]

53. Segraves WA, Hogness DS. The E75 ecdysone-inducible gene responsible for the 75B early puff in Drosophila encodes two new members of the steroid receptor superfamily. Genes Dev. 1990; 4:204–219. [PubMed: 2110921]

NIH-PA Author Manuscript

NIH-PA Author Manuscript

NIH-PA Author Manuscript

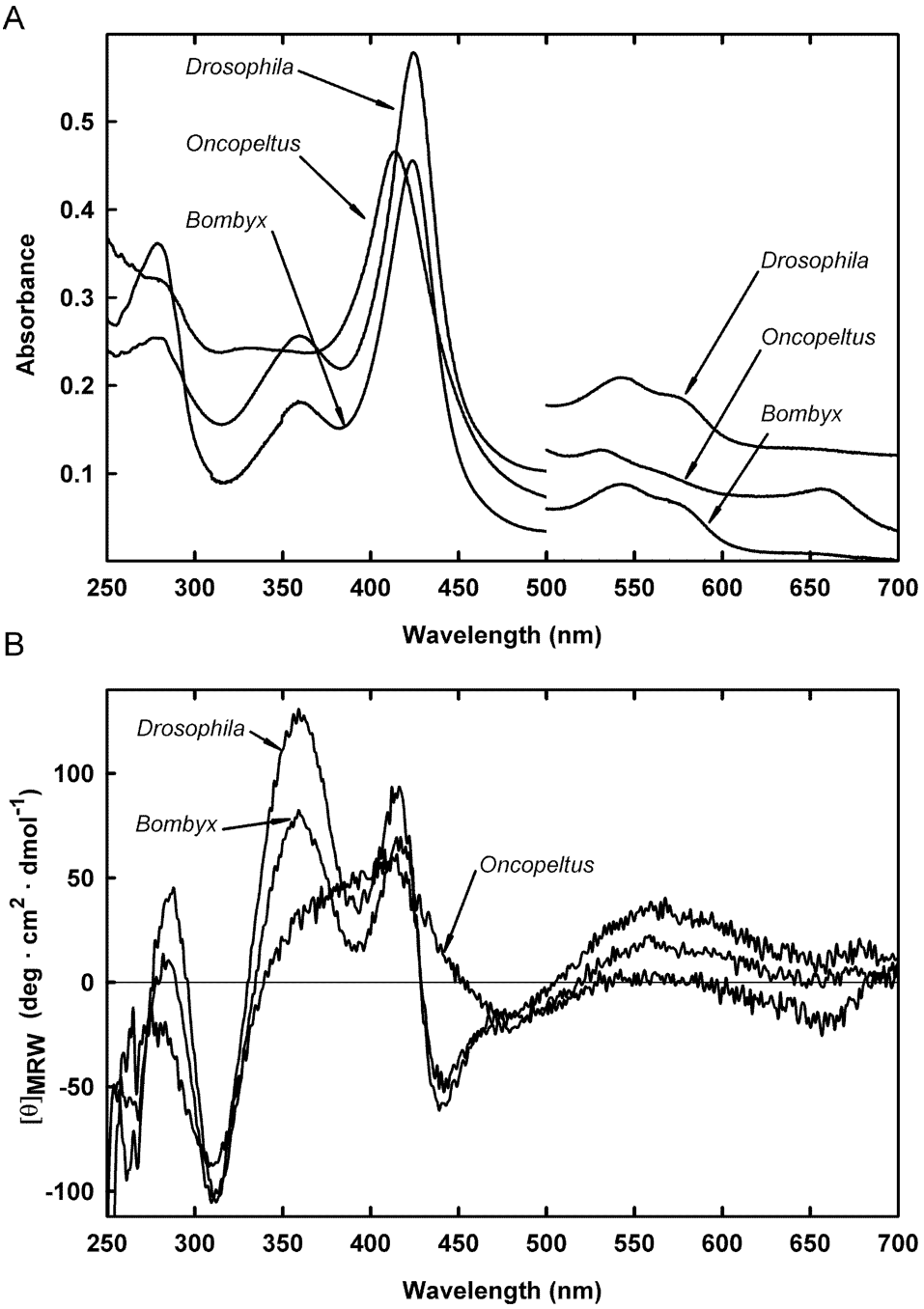

Figure 1. Characterization of the purified LBDs of three insect E75 proteins

(A) The absorbance spectra of the ferric forms of purified *Drosophila melanogaster*, *Oncopeltus fasciatus* and *Bombyx mori* E75 LBDs in the 250–700 nm. The spectra have been vertically displaced and the α/β bands (500–700 nm) magnified for clarity. (B) Circular dichroism in the near UV and visible regions of the purified E75 LBDs of *Drosophila melanogaster*, *Oncopeltus fasciatus* and *Bombyx mori*.

NIH-PA Author Manuscript

NIH-PA Author Manuscript

NIH-PA Author Manuscript

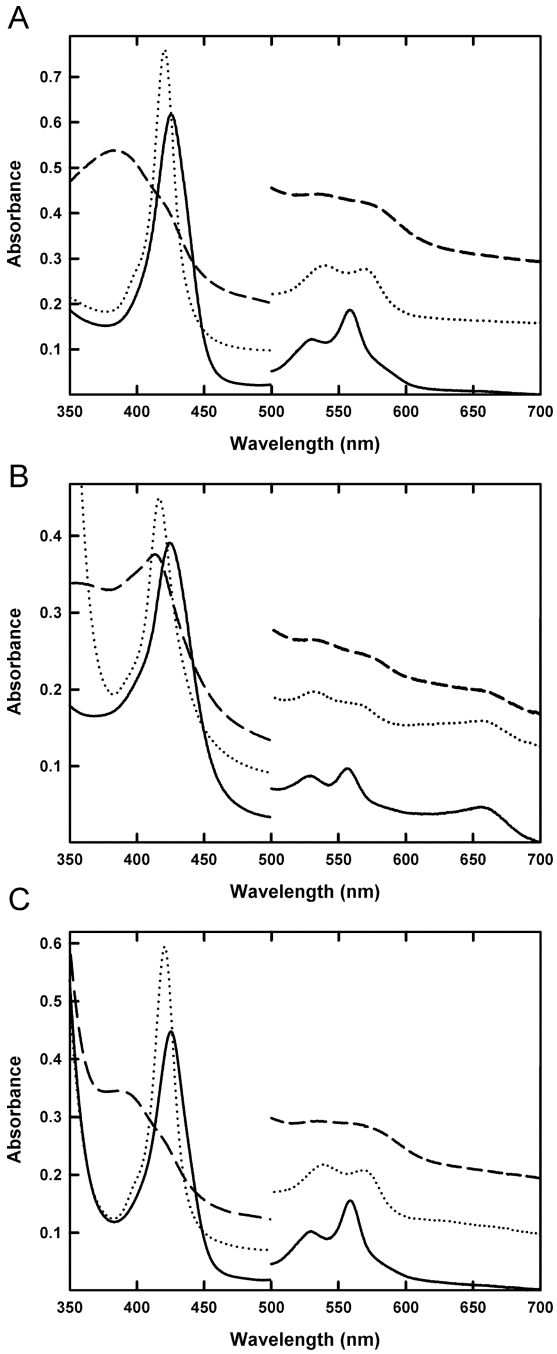

Figure 2. Anaerobic spectroscopic characterization of the ferrous forms of the insect E75 LBDs in the presence of ·NO and CO

The *Drosophila melanogaster* (A), *Oncopeltus fasciatus* (B) and *Bombyx mori* (C) E75 LBDs purified in the ferric state were subsequently reduced with sodium dithionite and the ·NO and CO complexes were formed anaerobically. The ferrous form is depicted with a solid line, the ferrous-CO complex with a dotted line and the ferrous-NO complex with a dashed line. The spectra have been vertically displaced and the α/β bands (500–700 nm) magnified for clarity.

NIH-PA Author Manuscript
NIH-PA Author Manuscript
NIH-PA Author Manuscript

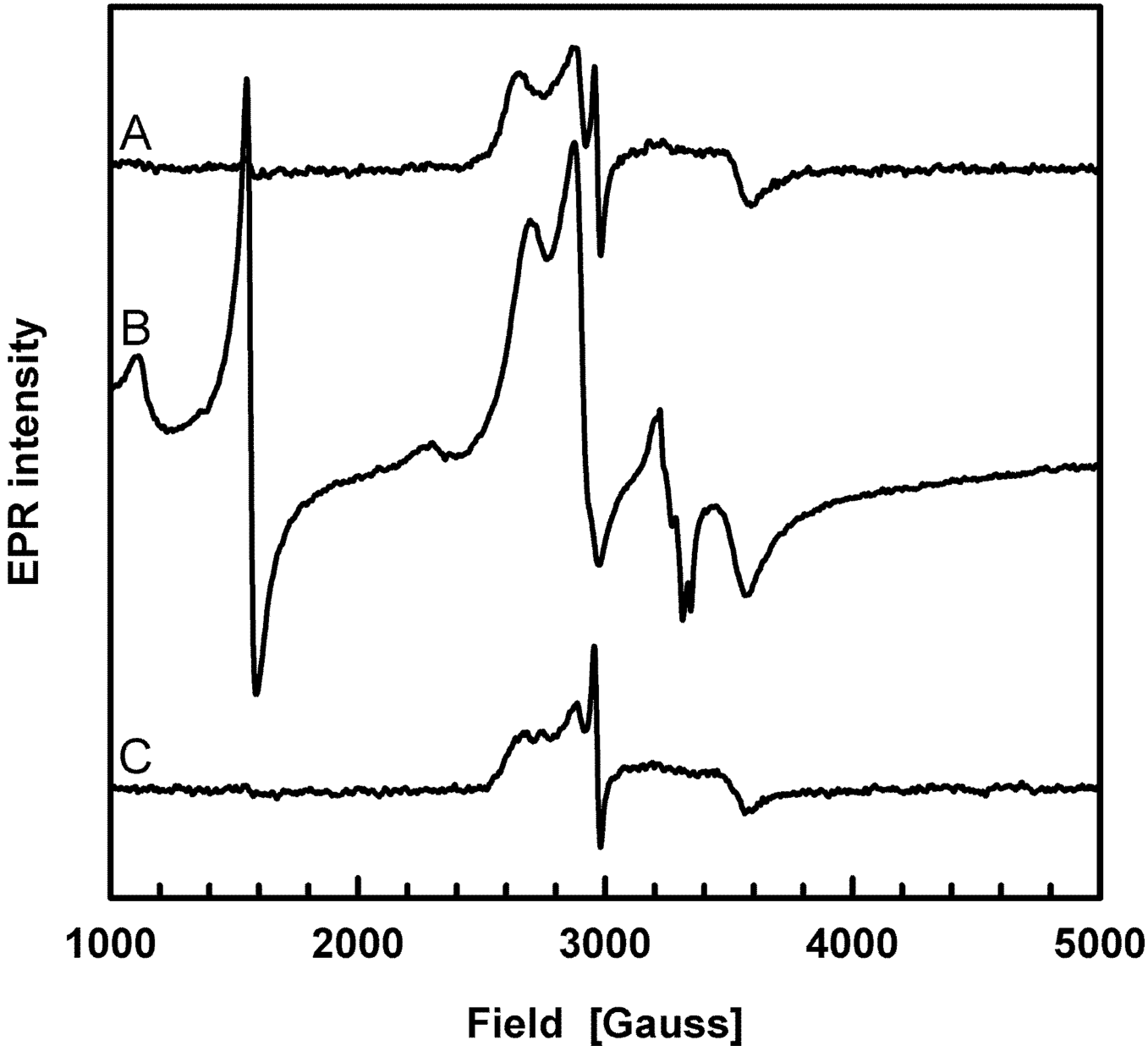

Figure 3. EPR spectra of the purified insect E75 LBDs

The spectra were recorded using the following experimental conditions: 50 mM Tris-HCl, 300 mM NaCl, and 8% (v/v) glycerol (pH 8.0); modulation frequency, 100 kHz; modulation amplitude, 1 mT; microwave power, 0.1 mW. (A) *Drosophila melanogaster* in the g ~ 2 region at 10.6 °K. (B) *Oncopeltus fasciatus* in the g ~ 2 region at 14 °K. (C) *Bombyx mori* in the g ~ 2 region at 10.6 °K.

NIH-PA Author Manuscript
NIH-PA Author Manuscript
NIH-PA Author Manuscript

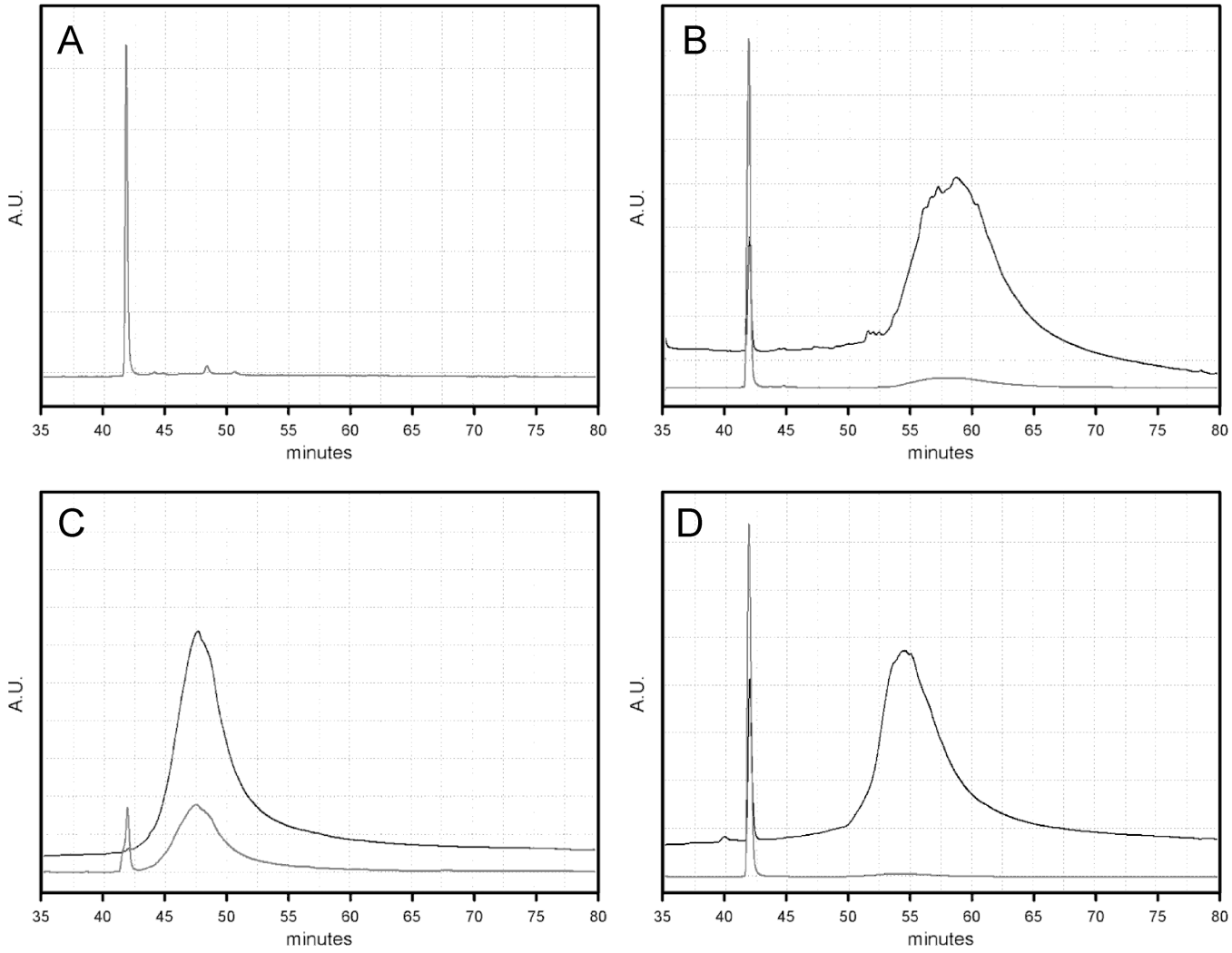

Figure 4. HPLC analysis of the purified E75 in a Beckman Coulter Ultrasphere C18 reversed phase column

The elution of the heme moiety (bottom traces) was determined at 400 nm whereas the protein (upper traces) was detected at 214 nm as described in the Materials and Methods section. An acetonitrile gradient was used to determine the elution position of free heme (A) as well as the elution of the *Drosophila melanogaster* (B), *Oncopeltus fasciatus* (C) and *Bombyx mori* (D) E75 LBD hemoproteins.

NIH-PA Author Manuscript

NIH-PA Author Manuscript

NIH-PA Author Manuscript

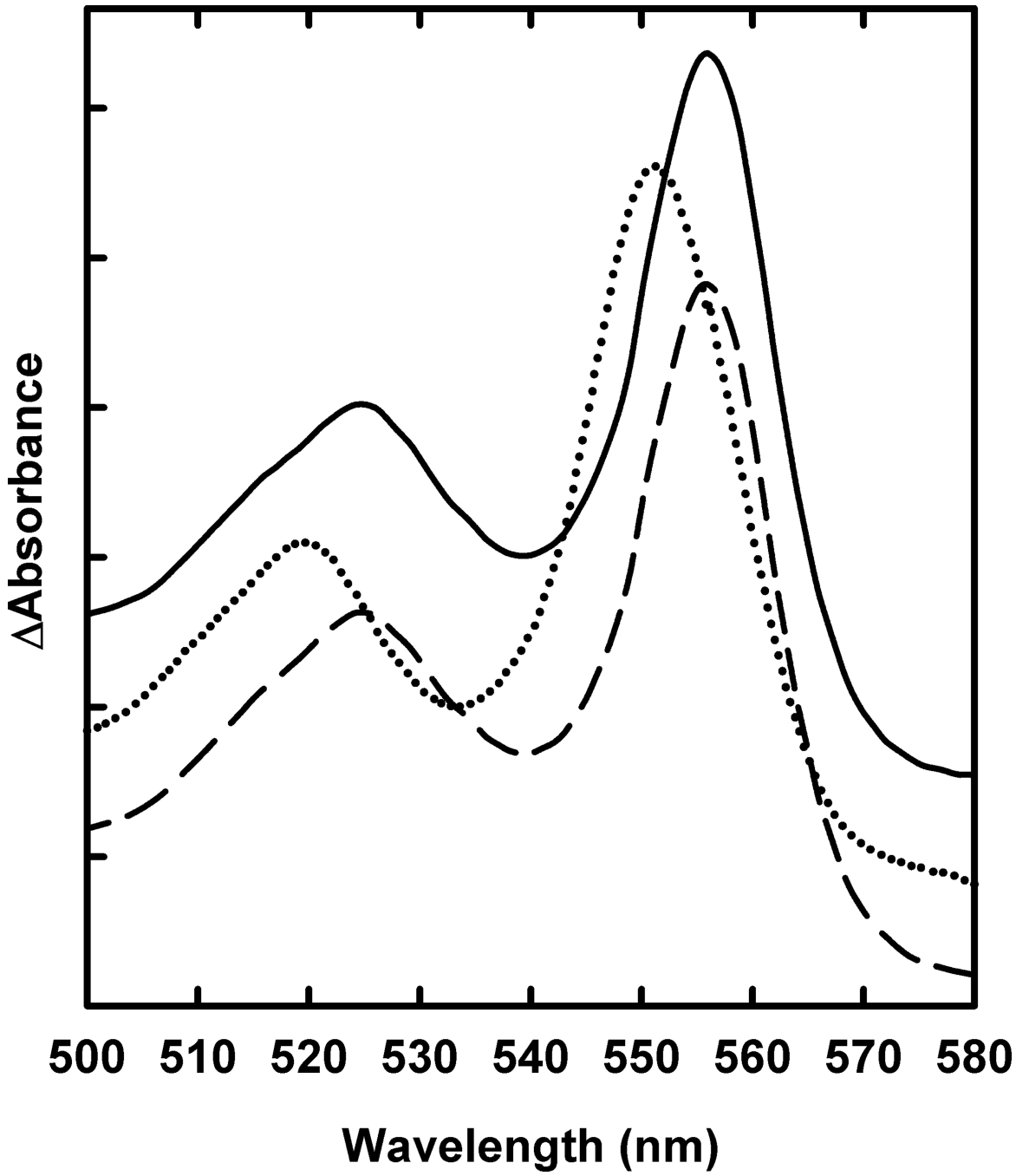

Figure 5. Pyridine hemochromes spectra of the insect E75 LBDs

The purified E75 LBDs of *Drosophila melanogaster* (solid line), *Oncopeltus fasciatus* (dotted line) and *Bombyx mori* (dashed line) were allowed to react with pyridine as described in the Materials and Methods section and the absorbance difference spectra were recorded between 500 and 580 nm. The spectra are vertically displaced for clarity.

NIH-PA Author Manuscript

NIH-PA Author Manuscript

NIH-PA Author Manuscript

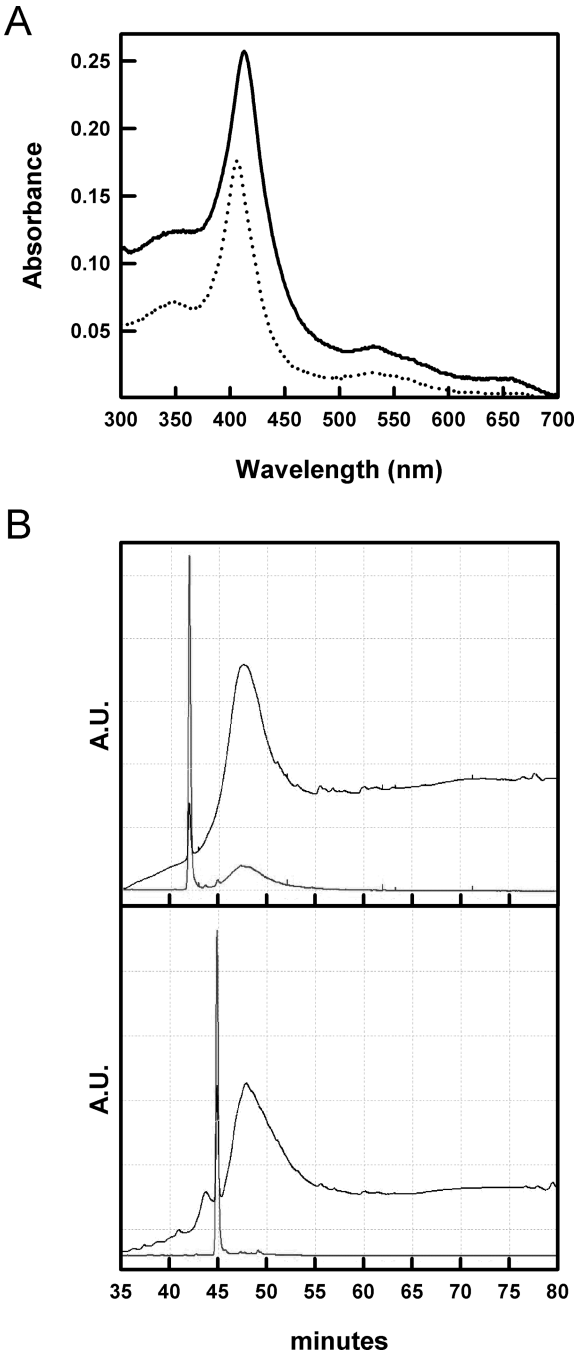

Figure 6. Spectroscopic and HPLC characterization of the *Oncopeltus fasciatus* E75 LBD recombinantly expressed in the heme synthesis-deficient strain RP523

(A) The absorbance spectra of ~24 μM *O. fasciatus* E75 LBD purified from bacteria supplemented with Fe(III) protoporphyrin IX (hemin) (solid line) or supplemented with Fe(III) mesoporphyrin IX (dotted line) are shown in the 350–700 nm range. The HPLC elution profiles (B) show the absorbance at both 214 nm (upper line) and 400 nm (bottom line). The elution profile of the *O. fasciatus* E75 LBD purified from bacteria supplemented with Fe(III) protoporphyrin IX (hemin) is shown in the upper panel whereas the elution profile of the *O. fasciatus* E75 LBD purified from bacteria supplemented with Fe(III)

mesoporphyrin IX is shown in the bottom panel. Free heme elutes at ~42 ml and free Fe(III) mesoporphyrin IX elutes at ~45 ml.

NIH-PA Author Manuscript
NIH-PA Author Manuscript
NIH-PA Author Manuscript

NIH-PA Author Manuscript
NIH-PA Author Manuscript
NIH-PA Author Manuscript

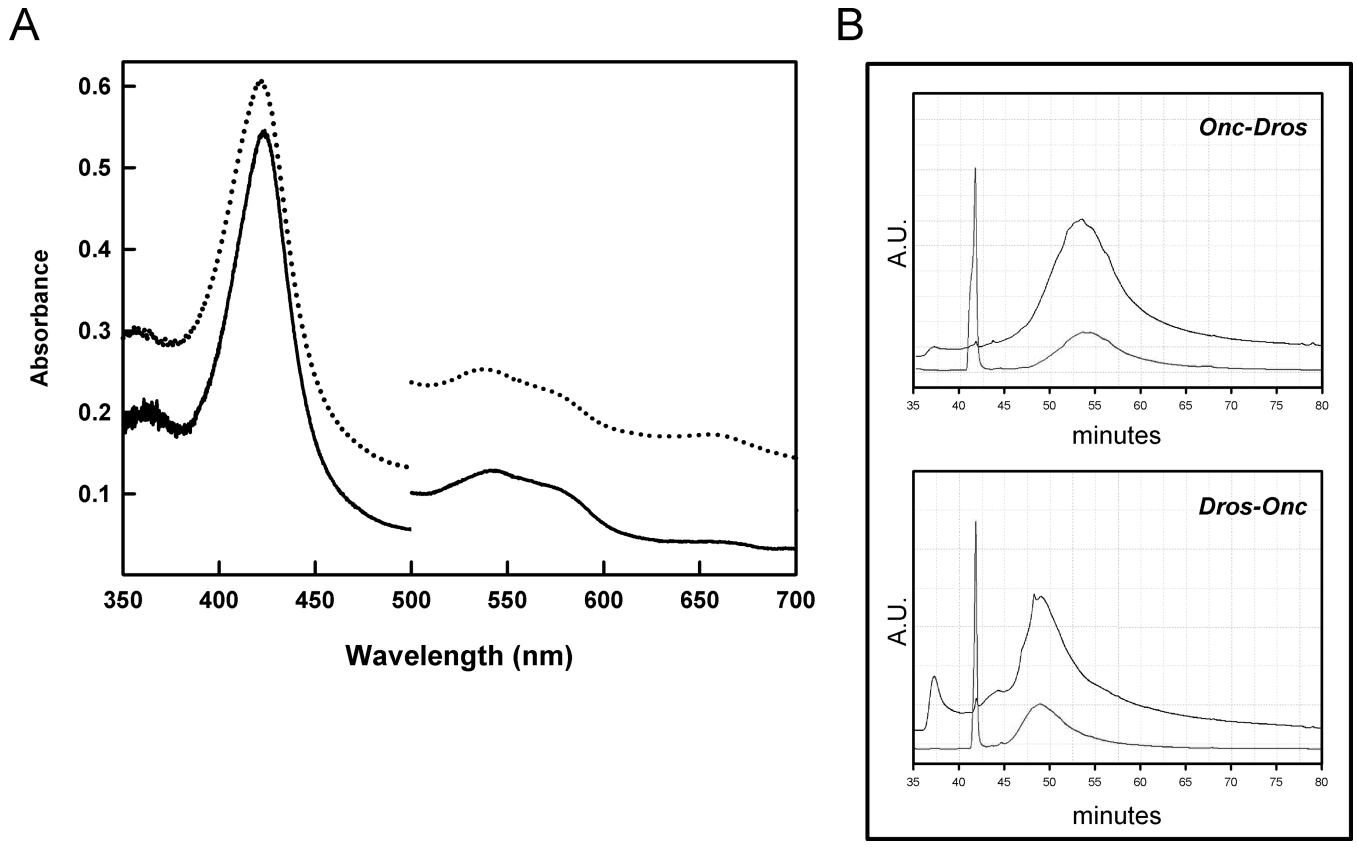

Figure 7. Spectroscopic and HPLC characterization of *D. melanogaster/O. fasciatus* E75 LBD chimeras

Chimeric constructs of *Drosophila melanogaster/Oncopeltus fasciatus* E75 LBD were made and purified from a bacterial expression system as reported in the Materials and Methods section (full sequences of the chimeras shown in Fig. S3). (A) The electronic absorbance spectra of the *Onc/Dros* (dotted line) and *Dros/Onc* (solid line) ferric form of the chimeras are shown in the 350–700 nm range. The 500–700 nm part of the spectra was magnified for clarity. (B) HPLC elution profiles of the *Onc/Dros* (upper panel) and *Dros/Onc* (bottom panel) chimeras both at 214 nm (upper line) and 400 nm (bottom line). In all cases free heme elutes at ~42 ml.

NIH-PA Author Manuscript
NIH-PA Author Manuscript
NIH-PA Author Manuscript

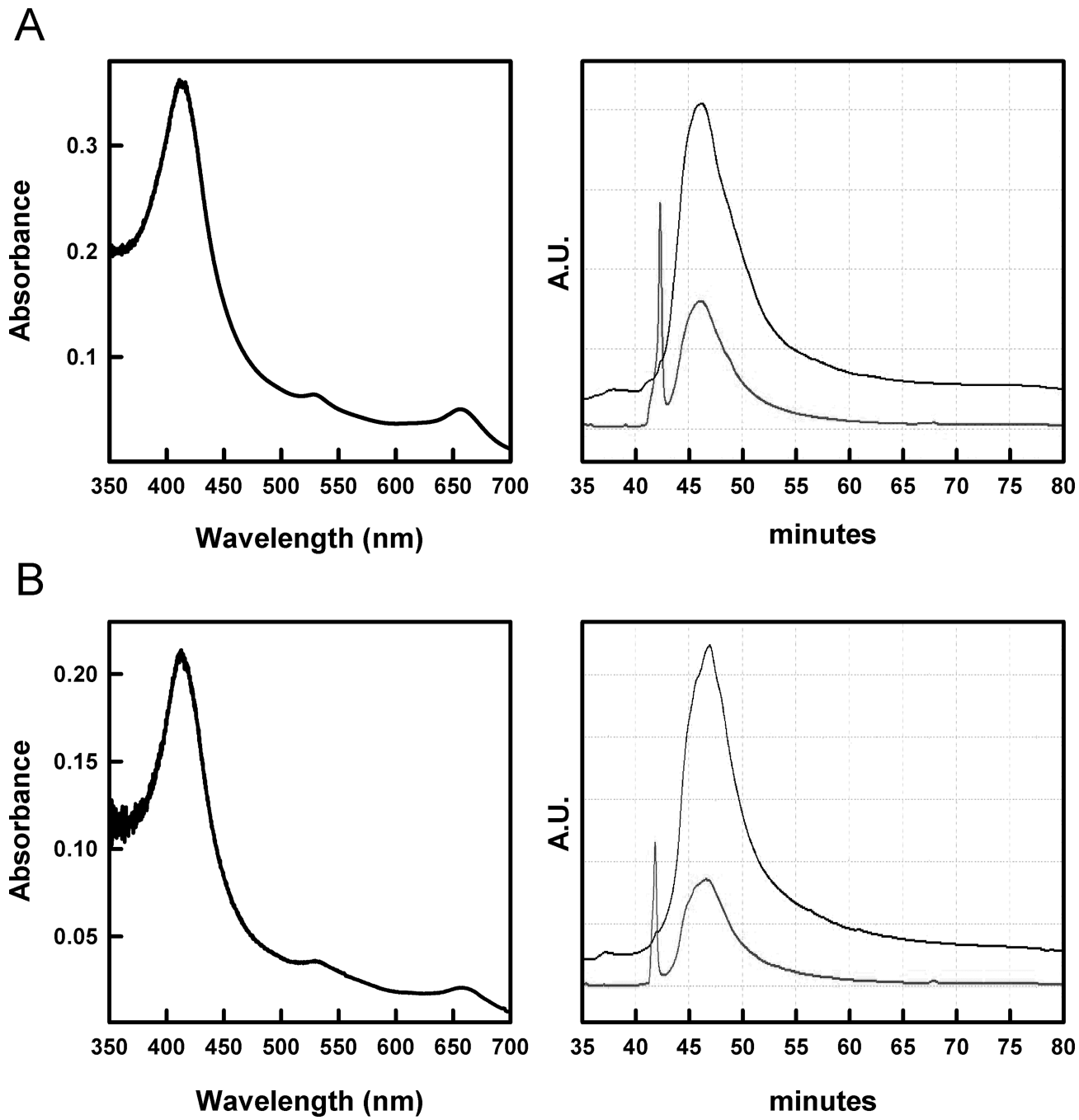

Figure 8. Spectroscopic and HPLC characterization of the *Oncopeltus fasciatus* E75 LBD Met245Thr and Glu158Lys mutants

Electronic absorbance spectra as well as HPLC elution profiles of the *O. fasciatus* E75 LBD Met245Thr (A) and Glu158Lys (B) mutants. The absorbance spectra are shown in the left panels in the 350–700 nm range. The HPLC elution profiles (right panels) show the absorbance at both 214 nm (upper line) and 400 nm (bottom line). In all cases free heme elutes at ~42 ml.

NIH-PA Author Manuscript

NIH-PA Author Manuscript

NIH-PA Author Manuscript

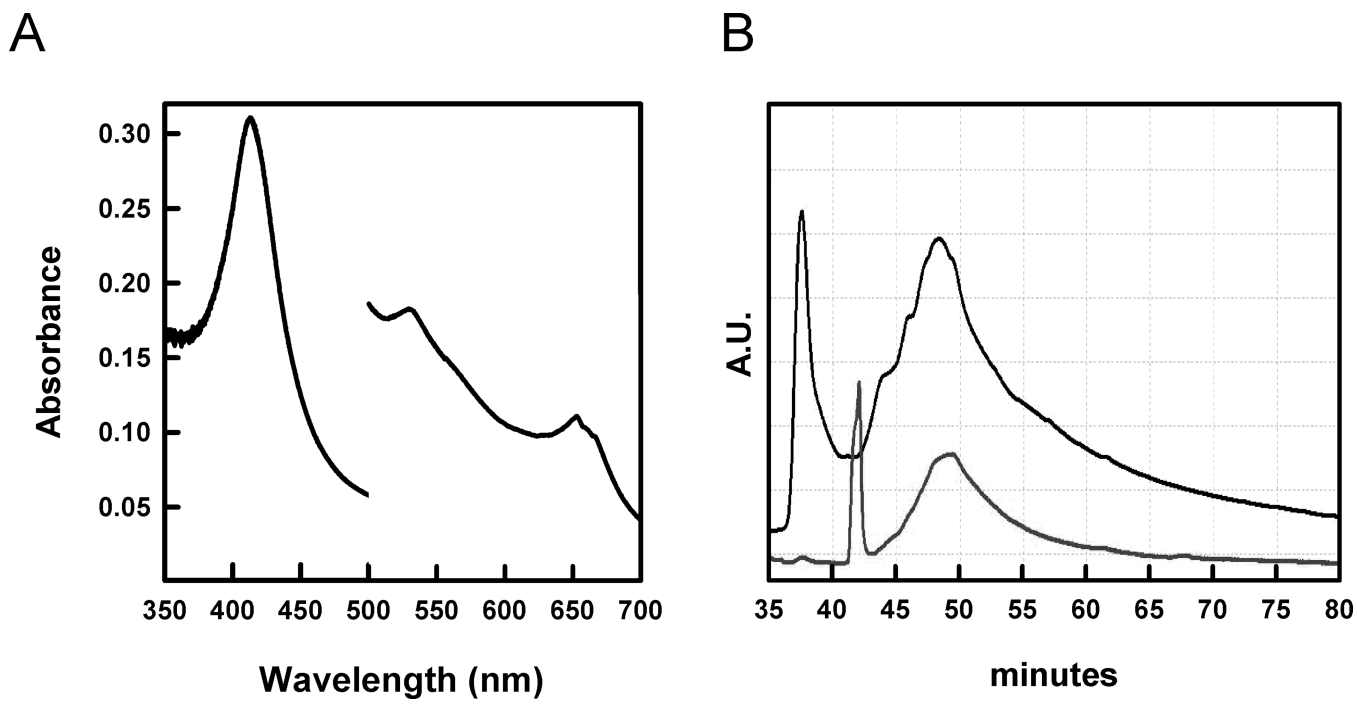

Figure 9. Spectroscopic and HPLC characterization of the *Blattella germanica* E75 LBD

Electronic absorbance spectrum (A) as well as HPLC elution profile (B) of the purified *B. germanica* E75 LBD. The absorbance spectrum is magnified in the 500–700 nm range for clarity. The HPLC elution profile shows the absorbance at both 214 nm (upper line) and 400 nm (bottom line). Free heme elutes at ~42 ml.

NIH-PA Author Manuscript
NIH-PA Author Manuscript
NIH-PA Author Manuscript

Table 1

EPR parameters.

EPR parameters								
sample	**spin**	**comp**[a]	**%**	**g1**	**g2**	**g3**	**V/Δ**[b]	**Δ/λ**[c]
Drosophila melanogaster	1/2	E1	~ 45	2.54	2.26	1.87	0.75	5.02
	1/2	E3	~ 55	2.33	2.26	2.04	1.19	6.92
Bombyx mori	1/2	E1	~ 30	2.54	2.26	1.87	0.75	5.02
	1/2	E2	~ 25	2.44	2.26	1.91	0.93	5.04
	1/2	E3	~ 45	2.33	2.26	2.04	1.19	6.92
Oncopeltus fasciatus	5/2		~ 10	6.02	2.92	~ 2.0		
	5/2		~ 40	4.32	2.28	~ 2.0		
	1/2		~ 20	2.48	2.27	1.88		
	1/2		~ 30	2.33	2.26	2.04	1.19	6.92

[a] Component of the EPR signal.

[b] Rhombicity.

[c] Tetragonal field.

NIH-PA Author Manuscript

NIH-PA Author Manuscript

NIH-PA Author Manuscript

Table 2

Amount of heme not associated with the protein moiety calculated after integration of the peak areas at 400 nm obtained from the HPLC analysis.

Amount of heme not associated with the protein moiety (% ± Std error)	
D. melanogaster E75 LBD	80.0 ± 2.1
B. mori E75 LBD	91.5 ± 3.9
O. fasciatus E75 LBD	8.9 ± 1.3
Chimera *Dros/Onc*	32.5 ± 0.1
Chimera *Onc/Dros*	35.0 ± 4.3
O. fasciatus E75 LBD Glu158Lys	10.9 ± 0.4
O. fasciatus E75 LBD Met245Thr	18.0 ± 0.2
B. germanica E75 LBD	16.9 ± 0.7